A Dissertation Report
On

Finite Element Analysis of Simply Supported Steel-Concrete Composite Girder Under Impact Loading

Submitted in Partial Fulfilment of the Requirements for the Award of Degree of

MASTER OF TECHNOLOGY
IN
STRUCTURAL ENGINEERING

Submitted by
ALOK
(2015PCS5152)

To

DEPARTMENT OF CIVIL ENGINEERING
MALAVIYA NATIONAL INSTITUTE OF TECHNOLOGY,
JAIPUR-302017-RAJASTHAN (INDIA)
APRIL 2016

A Dissertation Report
On

Finite Element Analysis of Simply Supported Steel-Concrete Composite Girder Under Impact Loading

Submitted in Partial Fulfilment of the Requirements for the Award of Degree of

MASTER OF TECHNOLOGY
IN
STRUCTURAL ENGINEERING

Submitted by
ALOK
(2015PCS5152)

To

DEPARTMENT OF CIVIL ENGINEERING
MALAVIYA NATIONAL INSTITUTE OF TECHNOLOGY,
JAIPUR-302017-RAJASTHAN (INDIA)
APRIL 2016

MALAVIYA NATIONAL INSTITUTE OF TECHNOLOGY JAIPUR

MALAVIYA NATIONAL INSTITUTE OF TECHNOLOGY JAIPUR

Certificate

I hereby certify that the work which is being presented in dissertation entitled **"Finite Element Analysis of Simply Supported Steel-Concrete Composite Girder Under Impact Loading"** is an authentic record of my own work carried out under the supervision of Dr Rajesh Gupta, Associate Professor and Dr Vinay Agrawal, Assistant Professor, in partial fulfilment of the requirements for the award of **Degree of Master of Technology** in **Department of Civil Engineering** from Malaviya National Institute of Technology, Jaipur for the year 2015-17.

Alok

(2015PCS5152)

IVth SEM, M. Tech.

This is to certify that the above statement made by the candidate is correct to the best of my/our knowledge.

Dr Rajesh Gupta
Department of Civil Engineering
MNIT, Jaipur

Dr Vinay Agrawal
Department of Civil Engineering
MNIT, Jaipur

ACKNOWLEDGEMENT

It is a matter of great pleasure and privilege for me to present this dissertation on **"Finite Element Analysis of Simply Supported Steel-Concrete Composite Girder Under Impact Loading"** I take this opportunity to express my deep sense of gratefulness and respect towards my guide **Dr Rajesh Gupta**, Department of Civil Engineering, Malaviya National Institute of Technology, Jaipur. I am very much indebted to him for the generosity, expertise and guidance which I have received from him working on this seminar and throughout my studies.

I would like to thank **Dr Gunwant Sharma**, Professor and Head of the Department of Civil Engineering, Malaviya National Institute of Technology, Jaipur for giving me this opportunity to do this work and all the staff members of the Department of Civil Engineering for their constant encouragement.

I would also like to express my gratitude towards **Dr Sandeep Choudhary, Mr Pankaj Kumar** for their effective and efficient guidance and P.G. Coordinator **Dr Vinay Agrawal** who helped me for the completion of my dissertation report.

Last but never the least sincere appreciations go to all my friends for their efforts and encouragement for successfully completing this work.

ALOK

(2015PCS5152)

IVth SEM, M. Tech

ABSTRACT

Steel-concrete composite girder is a common example of a composite structure used in civil engineering taking full advantage of compression capacity of the concrete and tensile strength of steel. In spite of the number of investigations on the steel-concrete composite girder, the effect of their dimension and detailing on their behaviour under impact loads has not been studied on a full-scale composite girder. Steel concrete composite girder exhibit peculiar behaviour under severe loading conditions associated with vehicular impact and impact generated by blasts. The evaluation of the behaviour of steel-concrete composite girder subjected to severe impact loads requires methods that can be used to analyse and design structures that will improve the state of the art of defensive design. The behaviour of steel concrete composite girder under impact loading has been studied numerically. This numerical simulation was aimed at characterising the dynamic behaviour of steel-concrete composite girder connected by headed shear connector under impact loading to prepare the base for a full-scale experimental test of the same under impact loading. This study presented an approach for numerical modelling of steel concrete composite girder under the effect of impact load, and a representative girder has been subjected to impact load to investigate the effects of the mass of impactor and drop height of impactor on the dynamic response and behaviour of the steel-concrete composite girder. Composite girder has been subjected to static and impact loads by three-dimensional simulations of the same using finite element analysis software package ABAQUS/Explicit, incorporating the parameters associated with the impact load and steel-concrete composite girder. The effects of mass and drop height of impactor on the behaviour and dynamic response of composite girder were numerically investigated. Impactors with mass of 20 tonne, 25 tonne, 30 tonne and 40 tonne has been dropped from heights of the impactor were 150 mm, 300 mm, and 600 mm over the midspan of composite girder. Various parameters such as acceleration, interfacial slip, velocity, stress, strain and support reaction have been recorded and compared with the case of static loading. The parameters such as acceleration, velocity, interfacial slip and support reactions showed great variation with the drop height of impactor while these parameters have not been significantly affected by the mass of impactor. Whereas, the stresses and strains produced in steel and concrete exhibited substantial variation with the variation of drop height as well as variation of mass of impactor. Sinusoidal variation of interfacial slip and reaction, reversed direction of reactions produced in the initial stages of impact is also noteworthy.

Table of Contents

List of Figures

List of Tables

CHAPTER 1

INTRODUCTION

1.1 General

In structural engineering, A structure is called composite structure when two or more than two materials are used to construct a structural element so that they act in unison. One of the common examples of such type of structure is when concrete slab is supported on steel beams. Compression capacity of concrete and tension capacity of steel is fully utilised by the steel-concrete composite construction. Owing to its fast construction, full utilisation of strength of materials, easy and sustainable disassembly steel-concrete composite structures are becoming a popular choice for over twenty years. The lightweight structure of composite elements has a huge advantage of reduced forces in supporting structure, including the foundations. The reduction in floor depth achieved by using composite construction has a considerable advantage in the form of the costs of building envelope and services. Composite constructions using normal weight concrete, have been used since 1920. Application of composite structures has ben seen in bridges since 1950 as a result of the research (Hegger and Rauscher 2007; Viest 1956). Implementation of composite structures in buildings was the result of the basic design provisions presented in the 1961 American Institute of Steel Construction (AISC) specification (King et al. 1965).

1.2 Composite Beam

In the case of composite construction using steel and concrete, the flange of I or T-shape steel beam is firmly attached with concrete slab using shear connectors. The resulting plate girder is proven to be more efficient than that of a plain steel plate girder due to the shift of neutral axis towards concrete through composite action between the steel girder and concrete slab (Baskar and Shanmugam 2003). The basic idea of the composite beam is the fact that the concrete is better in compression than steel (due to the absence of buckling as in the case of steel) and steel has better tensile strength. The advantage of both component material is successfully utilised by the composite action between steel and concrete. For the concrete part (within the effective width) of a cross section to resist compression, and the steel portion to carry tension, the two sections must be physically tied together. To resist external bending moment opposite nature of internal stresses (compressive in concrete and tensile in steel) have to be generated. This is accomplished by connecting both components using shear connectors. Generally, this attachment is achieved by ‘through deck welding’. A profiled metal decking to form the base of the composite slab is placed between the base of stud and flange of the steel beam (BCSA et al. 2001).

1.3 Connections

A shear transfer mechanism must be created between a steel beam and concrete slab to create composite action. In the absence of shear connection, steel beam and concrete slab would resist external forces as individual members. This way both of these components generate compression and tension zones of their own, and composite action is

not achieved. Hence the need for shear transfer mechanism between steel and concrete is generated to prevent the slip between the two components to achieve a composite action between the components of the beam (BCSA et al. 2001).

Headed Shear Connectors are mostly used for the steel-concrete composite beams and bridges. However, currently new types of shear connectors are often used, and studies have been carried out such shear connectors. A substitute shear connector called a perfobond strip, or more commonly known as a plate rib shear connector has been developed and studied in Japan, Europe, Canada, and Australia. The connector typically comprises a steel plate with holes, welded to the top flange of an I-section steel girder. During the casting of concrete, the holes are occupied by fresh concrete and the mutual action of shear strength of the concrete dowels (hardened concrete projections embedded in the holes of the steel plate), bearing action of the plate on the concrete and friction between components creates shear transfer mechanism between the steel and concrete slab. Stated advantages of this type of substitute shear connector are fabrication cost savings, negligible slip under service load and better safety due to the reduced trip hazards during construction. (Higgins and Mitchell 2001).

To facilitate fast erection of the composite structures hence to be able to be able to use precast concrete slab another type of connection has been used in which components can be adhered to each other on site by the use of epoxy resins and cement grouts. One of the advantages of this type of shear connection is that concrete slab bonded over steel is old enough to be free from shrinkage deformations. This process puts a limitation on the risk of cracking and thus contributes to durability (Jurkiewiez et al. 2011). Adhesive bonding also allows creating connection while avoiding major stress concentrations as they occur in joints when bolted or headed shear connectors are used.

In case if the replacement of concrete slab used in composite construction is required may be due to the end of the lifetime or may be due to an earthquake or accidental damage, bolted shear connectors comes with advantages of the easier dismantling of the structure. Prefabricated steel-concrete composite structures with bolted shear connectors can be used in commercial buildings, residential buildings, vehicle parking areas and modular building systems. They can be proved to be economical and efficient for short span crossing bridges and onsite assembled temporary bridges. Faster assembly and erection of such structures are achieved by embedding bolts in precast concrete slabs and in situ assemblies of the same into the already prepared flange of steel component of the composite girder. In this case, tolerances of prefabricated elements have to be minimised so as to achieve expected composite action of the structure. However, the construction using bolted shear connectors is costly when compared to headed shear studs. In spite of increased cost, faster assembly and life cycle cost analysis may be proved to be much more economical than the traditional methods of providing shear connections in composite structures (Pavlović et al. 2013).

Headed shear connectors are most common types of shear connectors used to resist horizontal shear and vertical uplift forces in steel-concrete composite girder. Headed shear

connectors (also referred to as the Nelson stud) prevents uplift and facilitates the shear transfer. Headed shear studs are also designed to work as arc welding electrode, and after welding, they facilitate the transfer of shear between steel and concrete and prevent uplift with a suitable head. As these type of studs are suitable for the automated fabrication process, they are preferred at a workshop or on the site (Pavlović et al. 2013). However, headed shear connector has a key role in the seismic response of the steel-concrete composite structure. They function as a key for composite action in bending as well as they can be used to transfer the large horizontal inertial forces generated in the slab to the main lateral load resisting member of the structure (Shariati et al. 2012). During an earthquake, such shear connectors are also subjected to reverse cyclic loading (Hawkins and Mitchell 1984). Furthermore, a recent global increase in events of terrorism and threats hints probable danger to the civil infrastructure, and thus impact and blast resistant design of structures have become a crucial obligation in the design processes (Pham and Hao 2016). Hence the analysis of composite structures is required under the extreme loading conditions.

1.4 Organisation of Thesis

1. Introduction

A brief introduction of composite structures and steel-concrete composite girder has been presented in this chapter. Further, some alternative methods to provide a connection between steel and concrete parts of girder has been discussed.

2. Literature Review

The previous studies pertaining to steel-concrete composite girder and impact load test on structures has been reviewed in this chapter. The research gap in the current studies has been revealed and based upon that gap an objective has been presented.

3. Methodology

This chapter deals with the methodology developed for modelling and analysis of steel-concrete composite girder under impact loading.

4. Numerical Validation

The methods of structural and material modelling developed has been numerically verified by their application in the previous studies. This chapter shows the consistency of the methodology developed with the help of previous numerical and experimental researches on the similar structures.

5. Results and Discussions

The results obtained from the numerical analysis of composite girder are precisely presented and discussed in this chapter with the help of tabular data and charts.

6. Conclusion

The conclusions formed on the basis of the results obtained along with the future scope of work are discussed in this chapter.

CHAPTER 2

LITERATURE REVIEW

2.1 Overview

An overview of the investigations on steel-concrete composite girder and analysis of impact load on structures has been presented in this section.

Wang (1998) studied the maximum deflection occurring in steel-concrete composite beams provided with partial shear interaction. In this paper, he developed a shear connector stiffness based method to calculate the maximum deflection occurring in composite beams. To validate this method, the computed maximum beam deflection using the method proposed is compared with the outcomes of a linear-elastic finite element analysis and experimental results of composite beams. A composite beam of span 9 m consisting concrete slab with depth 100 mm and width 2250 mm along with a universal steel section UB 305 × 127 × 37 was used as a representative to present results of the study. The Young's modulus of steel was adopted as 200 GPa, and same for concrete was taken as 20 Gpa. Wang (1998) also studied the effect of boundary conditions i.e. fixed, simply supported, three span continuous along with five load cases namely: (1) a point load at the centre; (2) a point load at ¼ span; (3) three equally spaced point loads; (4) uniformly distributed load over the full span; (5) triangular moment distribution between supports. Finally, Wang (1998) concluded that maximum deflection occurring in a composite beam with the partial shear connection might be calculated based on the stiffness of shear connectors by using given approach.

Thevendran et al. (1999) examined the behaviour of structural steel-concrete composite beam curved in plan. In this three-dimensional model, the concrete deck had been modelled using QUAD4 shell elements, the flanges of girder with BAR elements (comprising of torsional effects along with axial and bending strains in two directions), the web of girder using QUAD4 shell, and the shear connectors concrete slab and steel flange with RBAR elements (rigid in nature coupling all degrees of freedom of both to generate composite action). The concrete deck was assumed to be free from cracks throughout the bridge. Steel was assumed to be elastoplastic showing strain hardening nature in tension as well as in tension. The plastic region of the stress vs. strain curve was idealised as linear. Concrete under compression has been assumed to be elastoplastic material showing strain hardening. The strain at which concrete develops maximum compressive stress is taken as 0.002 whereas failure strain is adopted as 0.0038. The constitutive relation for the tensile behaviour of concrete is idealised a bilinear curve. The first part of bilinear curve starts from the origin and reaches up to maximum uniaxial tensile stress developed in concrete i.e. the strain at which concrete just starts cracking. The second part of the bilinear curve represents a linear softening model with the assumption that the tensile stress decreases with increase in tensile strain. After the attainment of maximum tensile stress tensile stress is assumed to deplete linearly to zero representing the softening of concrete due to the development of cracks. Thevendran et al. (1999) validated the finite

element model by comparing the calculated values with existing experimental results. The computed results obtained for beams of realistic proportion has observed to be in agreement with experimental results.

Liang et al. (2004) inspected the ultimate strength of continuous composite beams under the effect of combined shear and bending by using the finite element analysis method. The flanges, web and concrete deck slab has been modelled using four-node doubly curved shell element with reduced integration. Isolated shear stud connectors were modelled using three-dimensional beam elements. Concrete in compression comprising of strain softening behaviour is modelled by the equation proposed by Carreira and Chu (1985). The maximum compressive of concrete used is 35 MPa. Whereas, the strain produced at maximum compressive is adopted as 0.002. The linear elastic behaviour of concrete is assumed to exist up to the 40 percent of the maximum compressive. The constitutive relationship of concrete in tension is modelled based on the assumption that stress in concrete increases linearly with increase in strain up to maximum compressive stress, after which concrete starts cracking. After the occurrence of cracks in the concrete, the tensile stress decreased to zero following as the linear path as the concrete softens. The shear retention model is based on the assumption that the shear stiffness of open cracks depletes linearly to zero value as the opening of cracks is increased. To represent the isolated nature of stud shear connectors, they are modelled using three-dimensional beam element. To represent actual shear stud in terms of strength and stiffness the cross-sectional area of the stud is altered. The material behaviour of steel used in studs is idealised using a trilinear stress vs. strain curve. Elastoplastic model of steel along with strain hardening has been used in structural and reinforcement steel. Compression and tension stress vs. strain curves has been approximated using a trilinear curve. Liang et al. (2004) presented a design approach based on the finite element analysis result, which includes the effects of the composite action between steel beam and concrete slab, pullout failure of studs and shear buckling of web, and compared the same with experimental results and obtained good agreement between both.

Louw et al. (1970) were the first to report the behaviour of shear stud connector in steel-concrete composite construction under impact loading. Hard impact test has been conducted on pushout specimens with rising time tending to that of a gas explosion. Tests have been conducted on 12.7 mm diameter × 80 mm single connector non-decked and 16 mm diameter × 125 mm single shear connector decked specimens. Specimens have been subjected to static shear rate of 0.034 MPa/second to serve as a control for comparison. Whereas shear rates of 2 kN/ms and 227 kN/ms have been achieved by means of displacement control and guided drop weight respectively for hard impact, and the test parameters have been recorded at the intervals of 51 microseconds. In conclusions, Louw et al. found the shear rate and force experienced by the specimen to be less than the applied force due to the time lag. Further, the contribution of concrete in the dynamic strength has been found to be negligible.

Zheng et al. (2009) investigated the structural behaviour of concrete deck slabs under the application of static loads applied on patches in the bridges consisting composite girders by finite element analysis. A nonlinear 3D finite element analysis model was developed using ABAQUS software packages. In their study, Zheng et. Al. modelled supporting steel beams, diaphragms and concrete deck slab used in beam have been modelled using the shell element (S4R or S8R). The composite action was assumed to develop fully between steel beams and concrete deck slab, implemented using multipoint constraint between steel flange and concrete deck slab assuring nodal compatibility at the locations where constraints have been applied. The nonlinear behaviour of steel used as structural steel in beams and reinforcement steel has been implemented using a bilinear stress vs. strain response curve. The tensile behaviour of concrete has been implemented using the tension stiffening model. The post-failure behaviour of concrete is represented by a linear softening model in which the stress in concrete decreases to zero from a maximum value with increase in strain after generation of cracks. Concrete plasticity model is used to account for the nonlinear behaviour of concrete under compression. In conclusion, analysis results are discussed, along with inferences on the behaviour of the concrete deck slabs used in bridges are presented.

Kaewunruen and Remennikov (2007) demonstrated the implementation and development of a finite element model to compute the dynamic behaviour of prestressed concrete sleepers, especially under low-velocity impact loads generated by varying mass and height of impactor. Kaewunruen and Remennikov (2007) developed finite element using a finite element software package, LS-Dyna. Drop hammer impact machine has been used to generate a variety of impact loads by varying drop heights from 100 mm to 500 mm. The result parameters such as accelerations are recorded for the loads varying from 300 kN to 600 kN. In this investigation, the concrete used in the sleepers was modelled using an eight-node three-dimensional solid element. The behaviour of wires used for prestressing has been modelled using truss elements, to resist strain generated by prestressing forces. A perfect bond has been assumed between steel and concrete. The non-linear elastoplastic behaviour of concrete has been idealised by using a multilinear stress vs. strain curve. The nonlinear material behaviour of wire used for prestressing has been idealised using a bilinear, and multilinear isotropic stress vs. strain curve created using the data obtained from the manufacturer. From the experimental "contact load vs. time" chart, it can be seen that impulse lasted for about 7 ms. Finally, it has been concluded that ballast bed has a slight effect on the impact responses of prestressed concrete sleepers.

Zineddin (2008) studied the behaviour of concrete slabs under impact loading using numerical analysis and compared analytical results with that of experimental results. This study aimed at finding the effects of concrete slab reinforcement detailing on the dynamic behaviour and response of reinforced concrete slabs. The impactor has been dropped from the heights of 152 mm (6 inches), 305 mm (12 inches) and 610 mm (12 inches). Zineddin (2008) simulated the behaviour of the slab under the effect of impact loading using ABAQUS/Explicit incorporating the dynamic constitutive behaviour of steel and concrete. The concrete slab has been generated using one-inch three-dimensional eight-node brick

elements. The reinforcement steel bars have been created using two node beam elements with coupled motion to the adjacent concrete nodes thus creating a perfect bond between steel and concrete. The use of isolated beam elements is a comparatively more accurate method of modelling reinforcements because this method allows the calculation of stress in individual reinforcement. The Lagrangian formulation has been used for the elements in ABAQUS/Explicit which allows deformation of elements with the material. The elastoplastic material properties of steel have been modelled using isotropic strain hardening. Whereas, material properties of concrete slabs, has been modelled using the modified Drucker-Prager/Cap plasticity model. The bilinear stress-strain relation has been adopted for reinforcement steel used in steel frame and concrete. In the findings, Zineddin (2008) concluded that in most cases the numerical analysis over-estimated the loads generated during experiments by 40%. The increased rigidity of numerical model than the concrete used in experiments may be the reason of the overestimation of loads. Finally, Zineddin (2008) concluded that a better material model representing the concrete might lead to more accurate predicted responses when compared to experimental results. Furthermore, drop weight catching mechanism used in the explicit analysis should be improved to represent practical conditions more accurately.

Remennikov et al. (2010) presented the comparative analysis between results of experimental and numerical simulation of the response of square hollow section tubes filled with concrete and rigid polyurethane foam subjected to transverse impact loading. Dynamic three-point bending tests have been performed on the 100 × 100 × 5 square hollow section tubes to examine the impact response behaviour. Firstly, mild steel and stainless steel hollow tubes were subjected to dynamic three-point bending test later the test has been performed by filling the tubes with foam and concrete. The simply supported tubes were 2.5 m in length. Large support movements have been controlled using rebound mechanism. Direct impact load has been applied by dropping a 600 kg mass from a height of 650 mm. The acceleration at midspan and quarter-span has been measured using ‘shock accelerometers’ whereas the same has been measured at quarter span using ‘high-speed displacement laser sensor’. The displacement at midspan has been measured using ‘high-speed draw wire potentiometer’. The whole experiment is simulated through finite element analysis by using explicit dynamics non-linear finite elements software package. The model incorporates the components of experimental setup i.e. roller support along with rebound mechanism, steel tube filled with concrete and foam and a drop hammer. All the components except steel tube have been modelled using eight-node brick elements, whereas, ‘Belytschko-Tsay four-node thin shell elements’ has been used to create a tube. Only quarter of the drop weight and columns has been modelled because of symmetry in expected deformation and test setup. The model used for the steel in LS-DYNA requires yield stress, Poisson’s ratio and modulus of elasticity. In addition, an arbitrary curve for stress vs. strain is also required to model isotropic strain hardening of steel. Element size used for meshing has been taken as 10mm. The concrete infill used in tubes is modelled using ‘ continuous surface cap model’ in LS-DYNA. The continuous surface cap model can predict the response of concrete subjected to dynamic loadings such as vehicular impact and reversible cyclic loading. The parameters required in continuous surface cap

model can be generated using only basic material properties such as aggregate size, density and unconfined compressive strength.The contact between surfaces has been modelled to represent the contact generated during experimental analysis. '*CONTACT_AUTOMATIC_SURFACE_TO_SURFACE' algorithm has been used to specify contact properties between steel itself, drop hammer and steel tube, steel tube and the roller support and rebound mechanism. This type of contact property uses a particular value of friction between the contact surfaces and prevents penetration of the elements into each other. '*CONTACT_SURFACE_TO_SURFACE_TIEBREAK' algorithm is employed between the foam infill and steel tube in which the foam is permitted to slip, but separation is forbidden. Remennikov et al. (2010) concluded that numerical simulation models have been able to reasonably forecast the displacement history, failure modes and impact history for steel tubes filled with foam and concrete under the action of low-velocity impact.

Pham and Hao (2016) presented a review of Concrete Structures Strengthened with FRP Against Impact Loading. According to Pham and Hao (2016), impact test can be conducted by dropping a weight onto test specimens from a certain height. The impact event does not cause complete destruction of the test specimens but rebounds. The incident velocity of the impactor can be theoretically estimated by the equations of motion or experimentally determined by a high-speed camera, accelerometer, or an optical sensor. One of the advantages of this type of tests compared to Charpy and Izod pendulums is that a broader range of test geometries can be adopted. Although a semispherical impactor is commonly used in these tests, the use of other shapes such as cylinders or sharp point is possible. Dynamic capacities of the specimens can be determined by one blow drop-weight test while fracture energy is determined by multi-blow tests in which the specimens fail by a number of drops.

Kumar et al. (2017) carried out experimental investigations to provide a comparative analysis of the qualitative behaviour of adhesively bonded and mechanically connected steel-concrete composite connections. The experiments have been conducted on the push out specimens using drop weight hammer test. The 4.54 kg steel ball has been dropped from the heights of 457 mm and 1500 mm using a steel tube as a guide. The number of blows has been noted for each specimen for the initiation of a crack. In findings, Kumar et al. (2017) concluded that connection created with adhesive bond withstood more number of blows before the initiation of crack than that of the mechanical connectors. Whereas, the mechanical connection showed relatively more ductile failure.

Deng et al. (2015) mentioned collision impact as a cause of failure of bridges in a state-of-art review of the causes and mechanisms of the bridge collapse. Such impact can be generated due to a collision between vehicles and bridge superstructures. A large magnitude of localised impact force can generate the high magnitude of pressure causing damage to bridge components which may result in collapse. Moreover, energy generated from the collision can generate vibrations and inertial forces in the bridges.

A general skeleton for the analysis of a girder under impact loading has been developed with the help of the given literature. From the studies of Wang (1998) a general idea of composite section and strength of steel and concrete used in analyses can be derived. The studies of V. Thevendran et al. (1999), Liang et al. (2004), Zheng et al. (2009) has been used to develop methodology for the finite element analysis of steel-concrete composites that includes type of parameters required for material modelling of steel and concrete, types of elements used in modelling of the structure along with their effects on analysis. Research of Kaewunruen and Remennikov (2007), Zineddin (2008) gave an approximate idea of low-velocity impact loads such as the mass and height impactor to be used in the finite element analysis package. Studies of Remennikov et al. (2010) can be used to develop material modelling of steel and modelling of contact between different components of girder for the case of impact load application. Furthermore, review by Deng et al. (2015) reveals the severity of impact forces on bridge structures.

2.1 Research Gap

The literature review presented suggests the lack of methodology for experimental and numerical analysis of full-scale steel-concrete composite girder under the effect of impact loading. Currently, there has not been any investigation which deals with experimental setup and equipment for the application of impact load on the steel-concrete composite girder, may be due to the cost of such setup for impact load application over the full-scale girder, cost of materials and lack of skilled labour for the construction of full-scale steel concrete girder. These difficulties can be overcome by a preliminary numerical simulation of a full-scale steel-concrete composite girder under impact to get an approximation of behaviour and capacity of the same so that cost and labour for experimental analysis can be justified. The numerical simulation of the same can also be useful for the parametric study of the steel-concrete composite girder under the effect of impact loading.

2.2 Objectives

The fore mentioned research gap leads to the following objectives:

1. To develop a methodology of material and structural modelling of steel-concrete composite girder in a finite element software package for the numerical simulation of steel-concrete composite girder under the effect of the impact load.
2. Comparative analysis of the steel-concrete composite girder under static loading and the same subjected to variable impact loads generated by varying height and mass of impactor.
3. To study of variation of dynamic parameters such as midspan acceleration of concrete slab and bottom steel flange, the midspan velocity with time under the effect of variable load.
4. Comparison of maximum midspan deflection, interfacial slip between steel and concrete, total vertical reactions and stress vs. strain curve of steel and concrete generated due to static load with that of generated due to the application of impact load.

CHAPTER 3

METHODOLOGY

3.1 General

A number of finite element software packages are available for numerical simulation and analysis of structures used in civil engineering by taking the non-linear behaviour of materials into consideration. ABAQUS/Explicit 6.13 is one of such software packages used for the work presented in this thesis. The methodology developed for the numerical simulation and analysis of steel-concrete girder under impact load comprises of

1. Material modelling of concrete, steel for structural steel section, slab reinforcements and headed shear studs.
2. Structural modelling which consists of a general overview of the representative structure, 3D finite element modelling of concrete, structural steel section, slab reinforcements and headed shear studs along with the boundary conditions and constraint between these structural components.
3. Methods for load applications by varying loading parameters for the analysis of structure under various loading conditions.

3.2 Material Modelling

For the numerical analysis of the steel-concrete composite girder, ABAQUS requires certain material parameters which are discussed under material modelling for components above.

3.2.1 Concrete

In ABAQUS Modelling of concrete properties, it is necessary to analyse the linear and non-linear behaviour of Concrete. Crack propagation is a predominant source of nonlinearity and the main culprit for the ultimate failure of structures made from these materials. For Concrete Modelling, various constitutive models are proposed such as Smearing Cracking Model, Concrete Damage Plasticity method, Mohr- Coulomb Plasticity, Drucker-Prager models so much more to access non-linear behaviour of concrete. In concrete modelling, there is need to access the tensile and compressive behaviour of concrete under general loading. As Concrete is strong in Compression weak in tension, the equation for the stress-strain curve is to be provided for tensile behaviour and compressive behaviour. Cracking of concrete is considered to be the decisive phenomena for the representation of the behaviour of concrete. The constitutive model is dominated by cracking and post-cracking behaviour of concrete. For dynamic loading where degradation of the modulus of elasticity takes place, Concrete Damage plasticity model is used. The non-linear behaviour of concrete with cylindrical compressive strength 45 MPa having a modulus of elasticity (E_c) 36,380 MPa is modelled using 'Concrete Damage-Plasticity Model'.

3.2.1.1 Elastic behaviour of concrete

Initially, stress vs. strain curve under tension and compression loading is linear up to the elastic limit with its slope equals Modulus of Elasticity of Concrete (E_c). In ABAQUS, A linear elastic material model having Isotropic type is taken.

$$\sigma = \varepsilon * E_S \quad (3.1)$$

E_c is 36,380 MPa, and Poisson's ratio is 0.26

3.2.1.2 Concrete damage-plasticity Model (CDP)

The concrete damaged plasticity model implemented for the material modelling of the concrete slab in ABAQUS:

1. Enables modelling of quasi-brittle material such as concrete used for any type of elements such as solids, shells beams and trusses;
2. Makes use of the concepts of isotropic degradation of elasticity along with isotropic compressive and tensile plasticity to characterise the inelastic nature of concrete;
3. Can be implemented with reinforcement bar to model concrete reinforcement;

To fully implement CDP model in ABAQUS, the following mandatory parameters should be input

A. **Dilation Angle:** The magnitude of plastic volumetric strain generated during plastic shearing is controlled by the dilation angle and is assumed to be constant throughout the phenomena of plastic yielding. The angle of dilation is adopted as 36° (Kmiecik and Kamiński 2011).
B. **Eccentricity:** The rate at which the function tends to be asymptotic (the flow potential approaches to be a straight line as the eccentricity is reduced to a negligible value). The default flow potential eccentricity is 0.1, which implies that dilation angle of material is unchanged over a wide range of confining stress values.
C. $\mathbf{f_{b0}/f_{c0}}$ **:** The ratio of the ultimate stresses developed during uniaxial and biaxial compression. It adopted as 1.16 in this analysis (Kupfer and Gerstle 1973).
D. $\mathbf{K_c}$ **(shape factor):** The ratio of the second stress invariant on the tensile meridian, to that on the compressive meridian, at initial yield for any given value of the pressure invariant such that the maximum principal stress less than zero, it must be less than or equal to 1 and greater than or equal to 0.5. The default value is of K_c is (2/3).
E. **Viscosity Parameter:** It is a representation of the relaxation time of a viscoelastic system. The rate of convergence of the analysis in the softening region can be improved by using the viscoplastic alteration with a small value of the viscosity parameter (small as compared to characteristic time increment), without negotiating with the accuracy of the results. The value of viscosity parameter has been adopted as 0.00001 for the current analysis.

Two main failure mechanisms of concrete are the tensile cracking and the compressive crushing as assumed by CDP model used in ABAQUS.

3.2.1.2.1 Numerical model for compressive behaviour

In the concrete compression, the stress vs. strain curve created using the equations proposed by Carreira and Chu (1985) has been used to model the elastoplastic material behaviour of concrete considering strain softening after the appearance of cracks (Carreira and Chu 1985).

$$\frac{f_c}{f'_c} = \frac{\beta\left(\frac{\varepsilon}{\varepsilon'_c}\right)}{\beta - 1 + \left(\frac{\varepsilon}{\varepsilon'_c}\right)^{\beta}} \quad (3.2)$$

and

$$\beta = \frac{1}{1 - \frac{f'_c}{\varepsilon'_c \, Ec}} \quad (3.3)$$

For $\beta \geq 1.0$ and $\varepsilon \leq \varepsilon_u$

Where,

- $\mathbf{f'_c}$**:** Maximum stress typically referred as the compressive strength of concrete and obtained using procedures provisioned in ASTM C 39, Standard Test Method for Compressive Strength of Cylindrical Specimens.
- $\boldsymbol{\varepsilon'_c}$**:** Strain produced in concrete when the concrete reaches at its maximum value of stress.
  $\varepsilon'_c = (0.71 * f'_c + 168) * 10^{-5}$ (3.4)
- **β:** Material parameter influenced by the shape of the stress vs. strain curve.
- $\mathbf{f_c}$**:** Compressive stress corresponding to the compressive strain ε.

The following curve depicts the stress vs. strain graph obtained for f'_c.

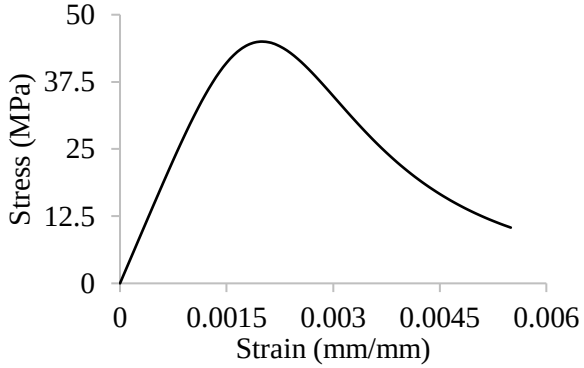

Figure 3.1 Actual stress vs. strain curve for plain concrete in compression

The stress- strain behaviour of concrete in compression has to be idealised for the development of a proper damage simulation model for the analysis of reinforced concrete deck slab under static and dynamic loading (Hibbitt et al. 2013). In the numerical modelling of concrete behaviour, 0.3 f′c is usually proposed as the limit of elasticity. (Chen 1988). Beyond this limit, the concrete material loses strength quickly. To define the stress-strain relationship, there is need to enter stress (f_c), inelastic strain (ε_{ie}) corresponding to stress values, and damage properties (d_c) (Wahalathantri et al. 2011). Further a corrective measure should be taken to ensure that the plastic strain values (ε_p) are neither negative nor decreasing with increased stresses (Hibbitt et al. 2013).

$$\varepsilon_{ie} = \varepsilon - \varepsilon_e \quad (3.5)$$

ε_e is the compressive strain corresponding to linear of elasticity i.e. 0.3 f'_c

$$d_t = \frac{\varepsilon_{ie}}{\varepsilon} \quad (3.6)$$

and

$$\varepsilon_p = \varepsilon_{ie} - \frac{dc}{1 - dc}\varepsilon_e \quad (3.7)$$

The following figure represents the idealised stress vs. strain graph for concrete under uniaxial compression.

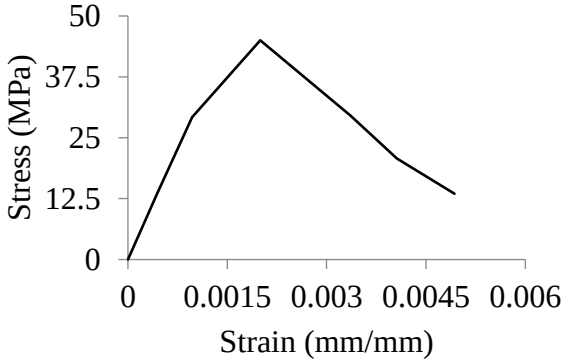

Figure 3.2 Idealised stress vs. strain curve of plain concrete in compression

3.2.1.2.2 Numerical model for tensile behaviour of concrete

Under the application of uniaxial tensile, the stress vs. strain of concrete can be idealised as a line originating from origin reaching up to a value of maximum tensile stress corresponding to the generation of the first crack due to the magnification of microcrack present in the interfacial transition zone of concrete. The generation of microcracks is represented macroscopically when the stress is increased beyond the failure stress representing the strain softening phenomena in concrete. The concrete under uniaxial

tension is modelled using the stress vs. strain curve created by the equations suggested by Carreira and Chu (1986) to represent its elastoplastic material characteristics.

$$\frac{f_t}{f'_t} = \frac{\beta\left(\frac{\varepsilon}{\varepsilon'_t}\right)}{\beta - 1 + \left(\frac{\varepsilon}{\varepsilon'_t}\right)^{\beta}} \quad (3.8)$$

- **β:** Parameter influenced by the shape of the stress vs. strain curve of concrete, taken same as in the case of concrete in compression (Carreira and Chu 1986).
- **f'_t:** Maximum tensile stress adopted as the 0.623 $(f'_c)^{0.5}$ (Committee et al. 2008)
- **ε'_t:** Strain required in concrete to produce maximum tensile stress, adopted as 0.1*ε'_c (Carreira and Chu 1986)
- **f_t:** Tensile stress corresponding to the tensile strain ε.

The stress-strain graph obtained for f'_c is obtained as given below

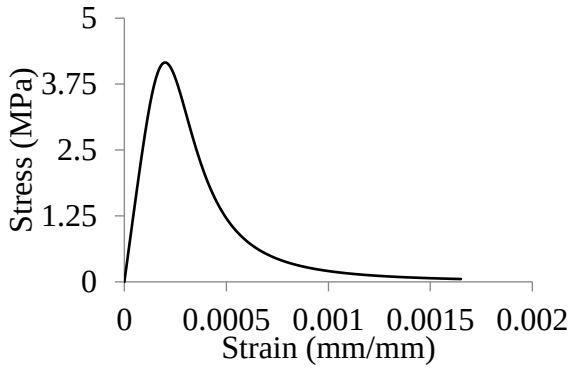

Figure 3.3 Actual reinforced concrete stress vs. strain curve in tension

The limit of elasticity is usualy adopted as 0.6 f'_t is in the numerical modelling of concrete. (Chen 1988). Beyond this limit, the concrete material loses strength quickly. To define the stress-strain relationship, there is need to enter stress (f_c), inelastic strain (ε_{ie}) corresponding to stress values, and damage properties (d_t) (Wahalathantri et al. 2011). Further a corrective measure should be taken to ensure that the plastic strain values (ε_p) are neither negative nor decreasing with increased stresses (Simulia 2013).

$$\varepsilon_{ie} = \varepsilon - \varepsilon_e \quad (3.9)$$

ε_e is the compressive strain corresponding to linear of elasticity i.e. 0.6 f'_t.

$$d_t = \frac{\varepsilon_{ie}}{\varepsilon} \quad (3.10)$$

and

$$\varepsilon_p = \varepsilon_{ie} - \frac{d_t}{1 - d_t}\varepsilon_e$$

(3.11)

The following curve depicts idealised stress vs. strain graph for concrete in tension.

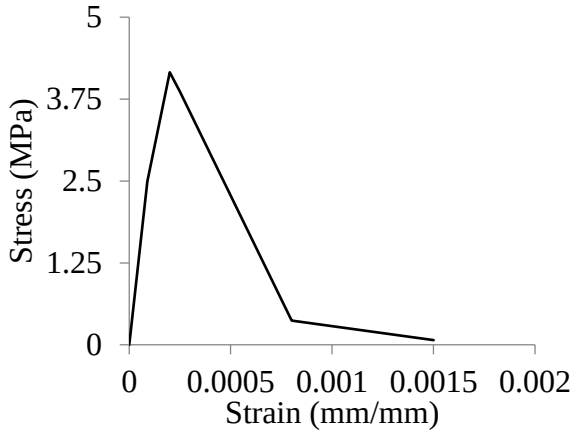

Figure 3.4 Idealised reinforced concrete stress vs. strain curve in tension

3.2.2 Steel

The details of steel used in the modelling of the full-scale steel concrete girder are summarised in the following table:

Part	Yield Limit (MPa)	Ultimate Strength (MPa)	Poisson's Ratio	Modulus of Elasticity (GPa)
Structural Steel	250	411.576	0.3	200
Reinforcement	250	411.576	0.3	200
Headed Shear Stud	351.63	448.16	0.28	209.187

Table 3.1 Details of Steel Used in Composite Girder

3.2.2.1 Elastic behaviour of steel

Initially, Stress- Strain curve under compression and tensile loading are linear up to the elastic limit with its slope equals Modulus of Elasticity of Steel (E_s). In ABAQUS, a linear elastic material model having Isotropic type is taken.

$$\sigma = \varepsilon * E_s$$

(3.12)

3.2.2.2 Plastic behaviour of steel

A kinematic/isotropic hardening model is implemented in ABAQUS to account for the non-linear plastic behaviour of steel such as strain hardening, Bauschinger effect.

3.2.2.2.1 Isotropic hardening of steel

For isotropic hardening, if a solid is deformed plastically, then unloaded and reloaded, an increase in stress required for yielding is observed as compared to that of in the first cycle. Such behaviour continues as long as the specimen reloaded beyond its maximum stress subjected during the previous cycle till the solid deforms plastically. Basically, isotropic hardening represents the behaviour in which, if the specimen is loaded in tension beyond the yield point, unloaded, then again loaded it in compression, yield will only be observed when it is loaded in beyond the maximum load reached in tension. Alternatively, isotropic hardening can be explained as the same amount of increase in yield stress of compression with the increase in the yield stress under tension due to hardening even though the solid might not have been subjected to the compressive load. Plasticity of ductile material can be implemented using this is a type of hardening used in material models for finite element analysis. Although, Isotropic hardening model cannot be used to accurately represent plasticity of real materials as it does not account for Bauschinger effect and accurate hardening of materials after few cycles.

3.2.2.2.2 Kinematic hardening of steel

The kinematic hardening models generally used to implement the behaviour of ductile materials subjected to reversed cyclic loading are independent of equivalent pressure stresses. These models can be successfully used to describe the plastic behaviour most of the metals subjected to cyclic loading, except voided metals (Hibbitt et al. 2013). The kinematic hardening models:

- Can be used to implement the inelastic behaviour of materials under the effect of cyclic loading;
- Consist of model linear kinematic hardening model as well as a nonlinear isotropic/kinematic hardening;
- Include a nonlinear isotropic/kinematic hardening model with multiple backstresses;
- Can be implemented in any analysis where elements with displacement degree of freedom are used;
- Can be applied to models where yield is dependent on rate of loading;
- Can be used in conjunction with swelling and creep; and
- Require the use of the linear elasticity material model to define the elastic part of the response.

In order to implement above-mentioned hardening model stress vs. strain data for steel under tension is required to input. Stress vs. strain curve for structural steel, reinforcements are from Atlas of stress-strain curves (Boyer 1987). The stress vs. strain curve for headed shear studs are obtained from experimental results available in literature (Kumar et al. 2017). The hardening region of the curve for structural steel and reinforcement is approximated using a trilinear curve.

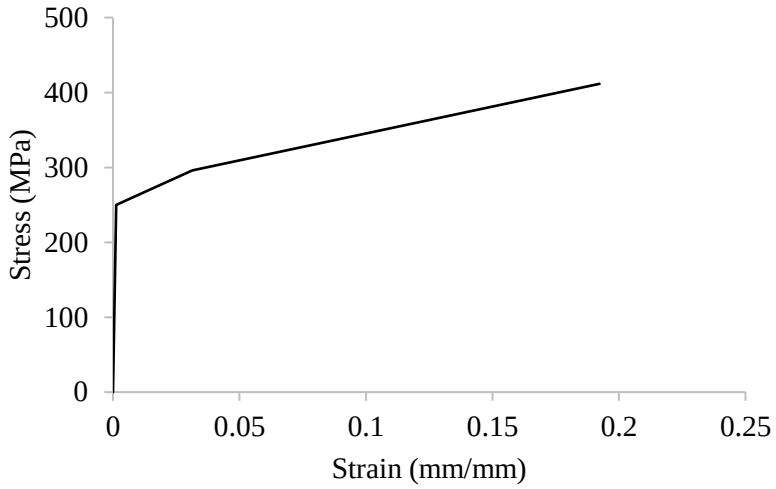

Figure 3.5 Stress vs. strain curve for structural steel

Whereas, hardening region of stress vs. strain curve for studs is approximated using a linear curve.

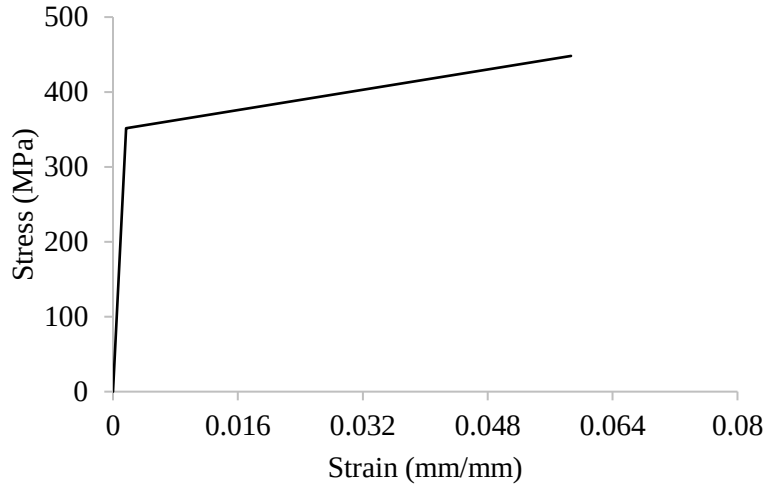

Figure 3.6 Stress vs. strain curve for shear stud

3.3 Structural Modelling

The physical implementation of the dimensions, shape, boundary conditions, assembly of the components, constraint between these structural components of the representative structure are required in ABAQUS to perform analysis of the representative structure. A general overview of the representative structure, physical modelling, 3D finite element meshing techniques are discussed under the structural modelling of the structure.

3.3.1 General overview of representative structure

The representative steel-concrete composite girder consists of a concrete slab (600 mm × 100 mm), I steel section (ISMB 350 (BIS 1964)) connected together by 20 pairs of uniformly spaced headed shear studs of diameter 15.875 mm. The concrete slab is provided with transverse reinforcement in the form of shear stirrups of 8 mm diameter bar with a spacing of 90 mm centre to centre, 5 number of 8 mm diameter bar as longitudinal reinforcements. A Clear cover of 15 mm and 23 mm is provided to transverse and longitudinal reinforcement respectively. The composite girder is supported on simple supports with an effective span of 5 m.

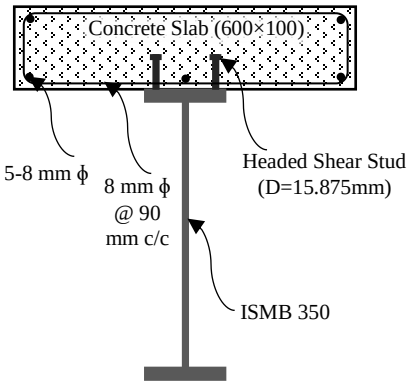

Figure 3.7 Section X-X of composite girder

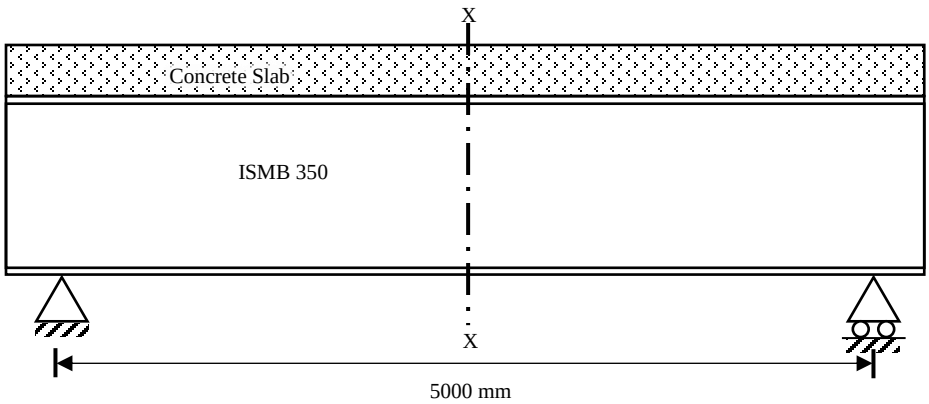

Figure 3.8 Elevation of composite girder

3.3.2 Finite element modelling of components

Shape, dimensions and type of elements are required to input in ABAQUS using certain modelling techniques. Implementation of such techniques is explicated under finite element modelling of components.

3.3.2.1 Concrete slab

A solid 3D type deformable concrete slab has been created using extrusion feature available in ABAQUS. For meshing ABAQUS provides a wide range of elements for different geometries and analysis types. For meshing of the concrete slab linear hexahedron type C3D8R (8-node trilinear brick) element is used, where R stands for reduced integration. Fast and cheap calculation of the element matrices can be achieved by reduced-order integration (mainly used by ABAQUS/Explicit), but it may generate a substantial amount of inaccuracy in results for a given problem.

3.3.2.2 Reinforcement

Reinforcement (both Transverse and Longitudinal) are created using 3D deformable wire shape. As the variation of stresses and displacements are not required in the cross section of the rebars, wire shape elements are computationally efficient.

3.3.2.3 I-Section

A solid 3D type deformable I-section is created using extrusion feature available in ABAQUS, by sketching a profile of the same. Web and flange portions are partitioned and separated by cuts using datum plane to ensure uniform mesh size and connectivity. For meshing of I-Section linear hexahedron type C3D8R (8-node trilinear brick) element is used.

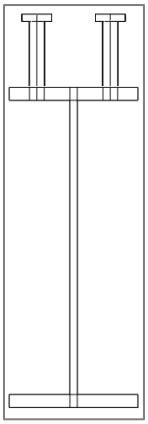

Figure 3.9 Partitioned I-section along with shear studs

3.3.2.4 Headed shear connectors

Headed shear connectors have been sketched and extruded over the top flange surface of I-section. This method of extrusion eliminates the need of tie constraint between the I-section and studs. Shear studs are difficult to mesh. Circular geometry of shear studs leads to the creation improperly proportioned elements during meshing. To overcome this problem, two diametric cuts are applied on studs, along with a small circular cut which is

extruded over the full length of the stud. While partitioning the studs in conjunction with the I-section, all the cuts are extended into the flange, and additional cuts are applied to separate interface of studs and flange in the form of a square. An additional circular cut equal to the leg diameter of the stud is applied. All the cuts applied to the studs are continued in the I-section to avoid discontinuity at the interface of stud and flange of I-section which may lead to poor meshing at their interface. A large number of shear connectors distributed over the flange of makes it difficult to apply the required cuts for each stud individually due to its repetitive nature. To solve this difficulty, required cuts has been automated using Python scripting feature of ABAQUS. The shear studs are also meshed using linear hexahedron type C3D8R (8-node trilinear brick) element.

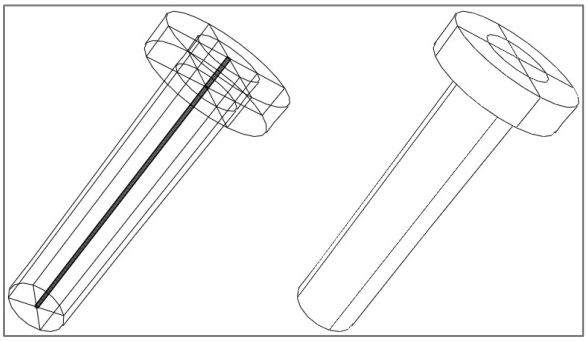

Figure 3.10 Wireframe and a solid view of shear stud with cuts

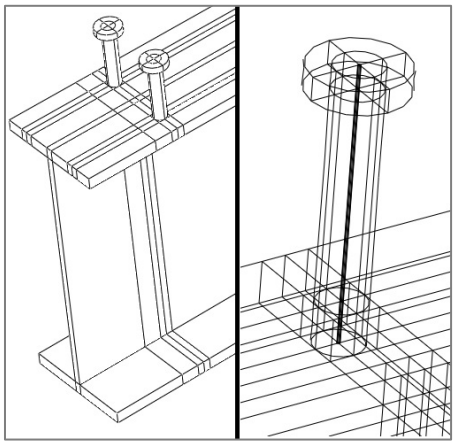

Figure 3.11 A view of extended cuts of studs into the I-section

3.3.2.5 Mass impactor

For the application of dynamic impact load, a discrete rigid 3D shell mass impactor is created using extrusion. The mass impactor is meshed using the linear quadrilateral element of type R3D4.

3.3.3 Boundary conditions, constraints, loading and analysis

Boundary conditions and nature and magnitude of the applied load are so adjusted that they represent the real time supports and loads over the structure. Techniques to implement the supports and loads over the structure are explained under this section.

3.3.3.1 Boundary conditions and constraint between components

To apply boundary conditions of simple supports, the composite girder is extended by 90 mm in both directions, so that horizontal slip of the girder over the roller of the simple support does not result in the collapse of the structure. Hinged end of simple support is modelled by restricting only displacements in all three directions on a line at the bottom of the flange of I-section at one end. Whereas, the roller support is modelled by restricting displacement only in vertical and transverse directions on a line at the bottom of the flange of I-section at another end of the girder.

For interaction between shear studs and concrete and reinforcement and concrete slab embedded region constraint is provided which helps in fully or partially eliminate degrees of freedom of a group of nodes and bind their motion to the motion of a master node (or nodes). Structural I-section comprising of twenty pairs of headed shear stud connectors and reinforcement act as embedded region embedded into concrete girder acts as host region.

A frictionless ‘General Contact’ interaction has been created between the composite girder and mass impactor which allows separation of surfaces after contact.

3.3.3.2 Loading and analysis

The impact strength of a composite member depends on both structural resistance and energy absorption capacity of the member. Impact test can be broadly classified into two parts: large mass with low velocity and small mass with high velocity. Large mass with low velocity include tests like drop-weight, Charpy test and Izod test. The drop-weight test is preferred over other methods of impact testing as it offers the highest flexibility regarding specimen geometry (Kumar et al. 2017).

The composite girder is loaded with static load at mid span to find its yield and collapse load, along with different parameters such as central deflection of the girder, longitudinal slip of girder over the roller support, stress and strain at the bottom of the flange of I-section and on the top of concrete at the mid-span, support reactions. The analysis of the girder under the static load performed using ABAQUS/Standard to establish a control for the comparison of obtained parameters with that of the girder under the impact load. All the loads are applied at the mid-span at the top of the concrete slab over an area of 600 mm × 800 mm.

Impact load is applied by providing velocity to a mass impactor (300 mm × 860 mm × 610 mm) and dropping it over a loading area at the mid-span of the girder. Masses of 20 tonne, 25 tonne, 30 tonne and 40 tonne each dropped from the heights of 150 mm, 300 mm, 600 mm. Dynamic explicit analysis is performed for a time period of 30 ms and parameters such as central deflection of the girder, relative slip between concrete slab and steel I-section over the roller support, stress and strain at the bottom of the flange of I-section and on the top of concrete at the mid-span, support reactions, acceleration and velocity at bottom midspan of girder are recorded.

CHAPTER 4

NUMERICAL VALIDATION

4.1 General

The methodology developed for the material and structural modelling has to be verified for its consistency by its application to the previously published analysis of structures either experimental or numerical. This section comprises of verification of properties of material and structural modelling of steel and concrete by comparing results obtained from numerical simulation of structures in ABAQUS 6.13 with the numerical or experimental analysis results of similar structures.

4.2 Numerical validation of steel modelling

A partially restrained unbraced frame (Foley and Vinnakota 1997) has been modelled and analysed using ABAQUS/Standard by the application of gradually increasing static load. The details of dimension and the load application is given in the following figure.

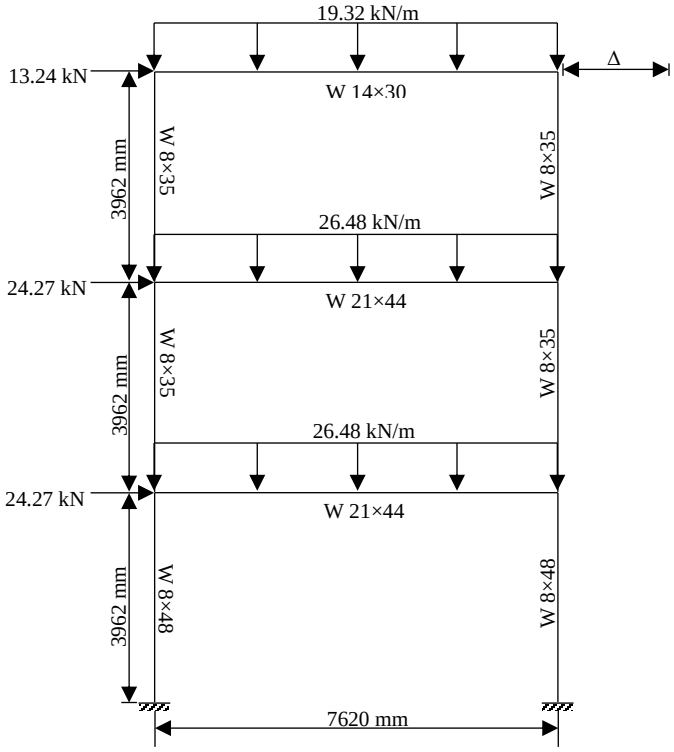

Figure 4.1 Loading arrangement on frame

Section	H	W	t_f	t_w
W 8 × 48	215.9	206.99	17.4	10.16
W 8 × 35	206.25	203.71	12.57	7.87
W 21 × 44	525.78	165.1	11.43	8.89
W 14 × 30	351.54	170.94	9.78	6.86

Table 4.1 Dimensions of I-section (mm) used in frame

Steel used in the frame is having a yield stress of 250 MPa and modulus of elasticity as 200 GPa. The load has been applied in factors of the shown load in figure 4.1 and deflection of top right corner of the frame is noted. The results (load factor vs. deflection) obtained are compared with that of from the analysis of Foley and Vinnakota (1997).

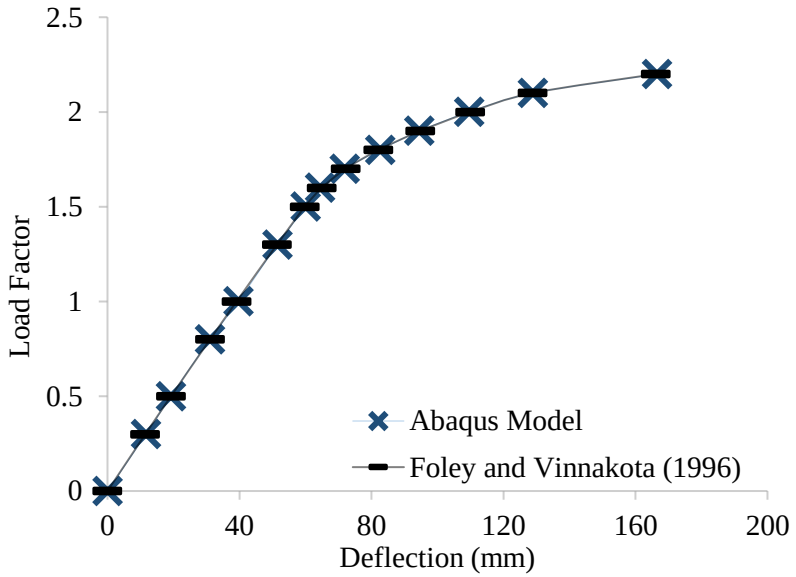

Figure 4.2 Load factor vs. deflection curve for frame

As it is clear from the graph that the load factor vs. deflection graph from ABAQUS model is coinciding with the graph as per previous analysis, it can be concluded that the properties used for steel are satisfactory and can be used for further analysis.

4.3 Numerical validation to reinforced concrete modelling

For the verification of reinforced concrete properties, a reinforced concrete girder (Song et al. 2002) consisting three similar T-beams has been modelled in ABAQUS and results are matched with the experimental results. The mean values of the the compressive strength and initial elastic modulus of concrete used in T-beam bridge are 35.3 MPa and 26,470, respectively; yield stress of the reinforcement bar used is 435.8 MPa. Dimension and reinforcement details of a T-beam girder and loading arrangement are shown in the following figures.

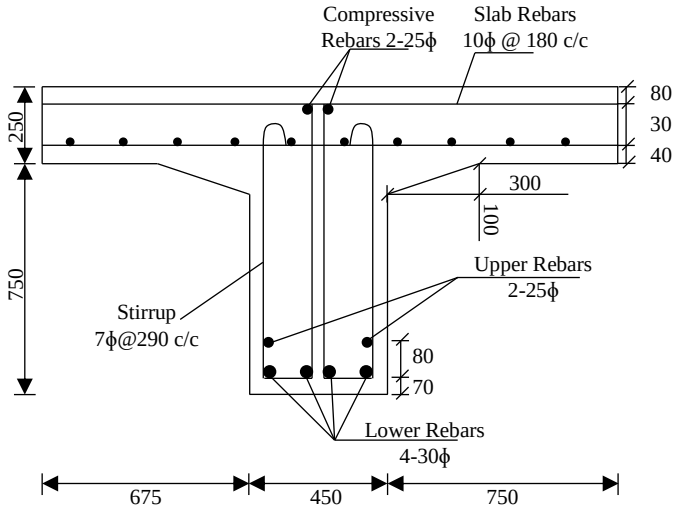

Figure 4.3 Reinforcement details of T-beam girder (all dim. in mm)

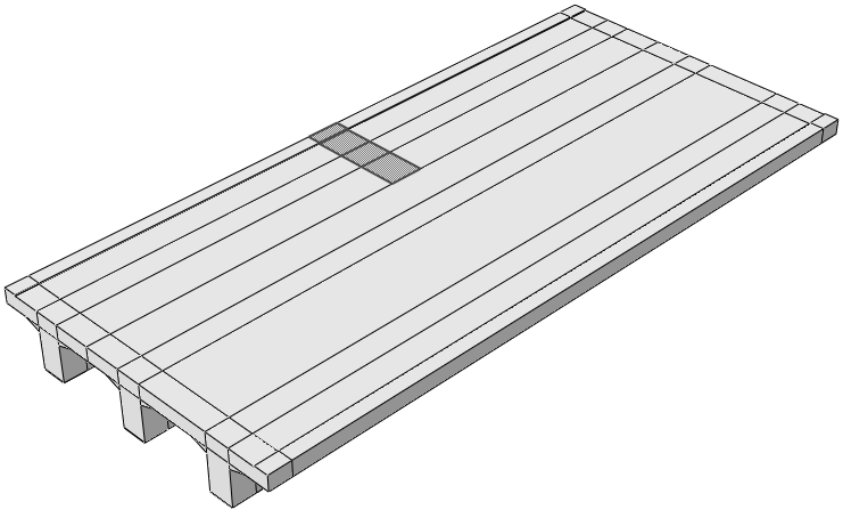

Figure 4.4 Highlighted loading area (1875 mm × 600 mm) on T-beam bridge

For the target bridge, concentric loading at the centre of the span is imposed along one line at the centre of the span so as to simulate a three-point bending condition. A load vs. deflection curve is plotted from the analysis results of the ABAQUS and matched with the experimental results.

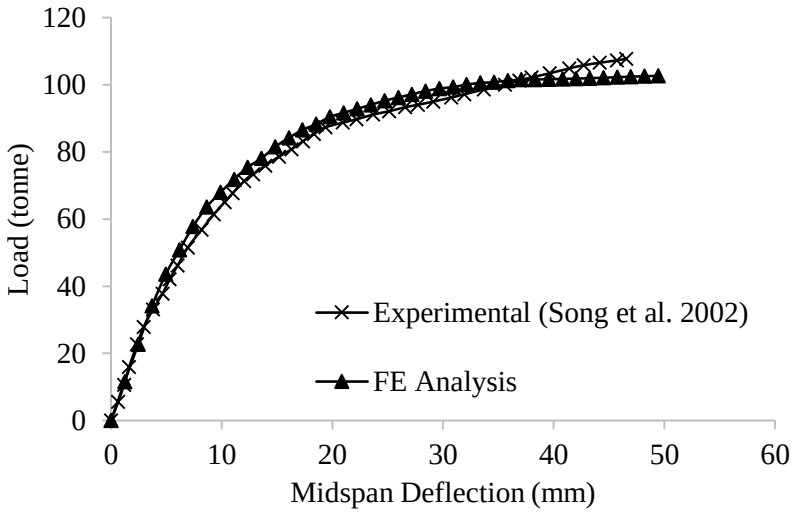

Figure 4.5 Load vs. midspan deflection curve for T-beam bridge

As it is clear from graph load vs. deflection curve obtained by finite element analysis is closely following the curve obtained by experiment on T-beam bridge. From the above curve, it can be concluded the material properties used for reinforced concrete are closely resembling the actual material properties and can be used hence these properties can be used for further analysis.

CHAPTER 5

RESULTS AND DISCUSSIONS

5.1 General

The behaviour of the steel-concrete composite girder with respect to different parameters recorded under static and impact loading analysis are compared and provided with possible explanations of such behaviour are presented in this section.

5.2 Static Analysis

By rigid plastic analysis, the theoretical collapse load of girder for same loading conditions is calculated as 324.52 kN. The representative girder is loaded with gradually increasing the static load until collapse. The collapse load for the girder is found to be 305.13 kN, whereas the yield load of the girder is found to be 231.62 kN. The collapse load reached 94.03% of theoretical collapse load computed by rigid plastic analysis. Reduction in collapse load by numerical analysis as compared to the rigid plastic analysis may be due to the fact that the cross section of composite girder was not fully yielded across the depth of the girder as assumed in the theoretical analysis.

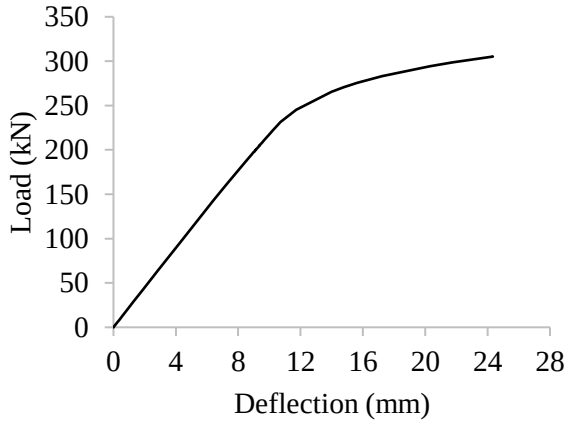

Figure 5.1 Load vs. midspan deflection of composite girder

The ultimate midspan deflection of the composite girder is found to be 24.34 mm.

The Stress vs. Strain curve for steel I-section at the midspan of bottom flange is given bellow.

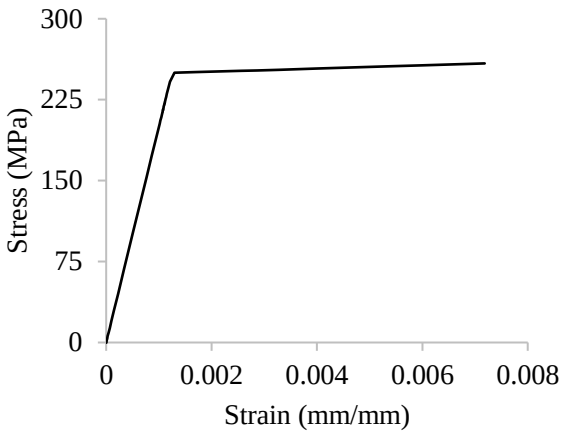

Figure 5.2 Stress vs. strain curve for steel at midspan of the bottom flange

The Stress vs. Strain curve shows yielding of steel as the longitudinal stress at the midspan of the bottom flange increases beyond yield limit of the steel due to the applied load.

The Stress vs. Strain Curve at the top of the concrete slab is shown in the following chart.

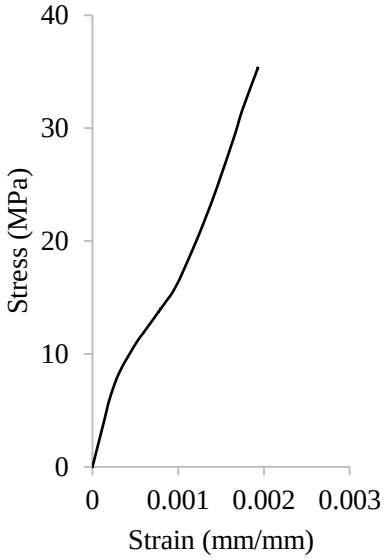

Figure 5.3 Stress vs. strain curve for top of concrete slab at midspan

The Stress vs. Strain curve for concrete shows the non-linear behaviour of concrete from the start with a maximum longitudinal compressive strain of 0.00193 corresponding to a maximum stress of 35.34 MPa.

5.3 Impact Load Analysis

For comparison of the behaviour of composite girder with impact load, impactor of mass 20 tonne (<yield load), 25 tonne (>yield load), 30 tonne (>yield load) and 40 tonne (>collapse load) are used. The parameters corresponding to equivalent static loads are given in the following table.

S.N.	Parameters	200 kN	250 kN	300 kN	Ultimate Load
1.	Midspan deflection at the bottom flange of the steel I-section (mm)	9.13	11.72	21.74	24.34
2.	Midspan deflection at the top of the concrete slab (mm)	9.13	11.72	21.74	24.34
3.	Midspan stress at the bottom flange of the steel I-section (MPa)	216.16	250.61	256.80	258.61
4.	Midspan stress at the top of the concrete slab (MPa)	13.78	16.80	31.60	35.34
5.	Midspan strain at the bottom flange of the steel I-section	0.00108	0.00170	0.00598	0.0072
6.	Midspan strain at the top of the concrete slab	0.00075	0.00103	0.00175	0.0019
7.	Relative slip between concrete slab and top flange of steel (mm)	0.02733	0.04425	0.06816	0.07026
8.	Total vertical reaction at simple supports	200	250	300	305.13

Table 5.1 Parameters for static analysis

The behaviour of steel-concrete composite girder under the impact loading in light of various parameters obtained by finite element software package for varying mass of impactor and drop heights are described in following sections.

5.3.1 Variation of midspan acceleration at the bottom steel flange

The following curves show the variation of midspan acceleration at the bottom of steel flange.

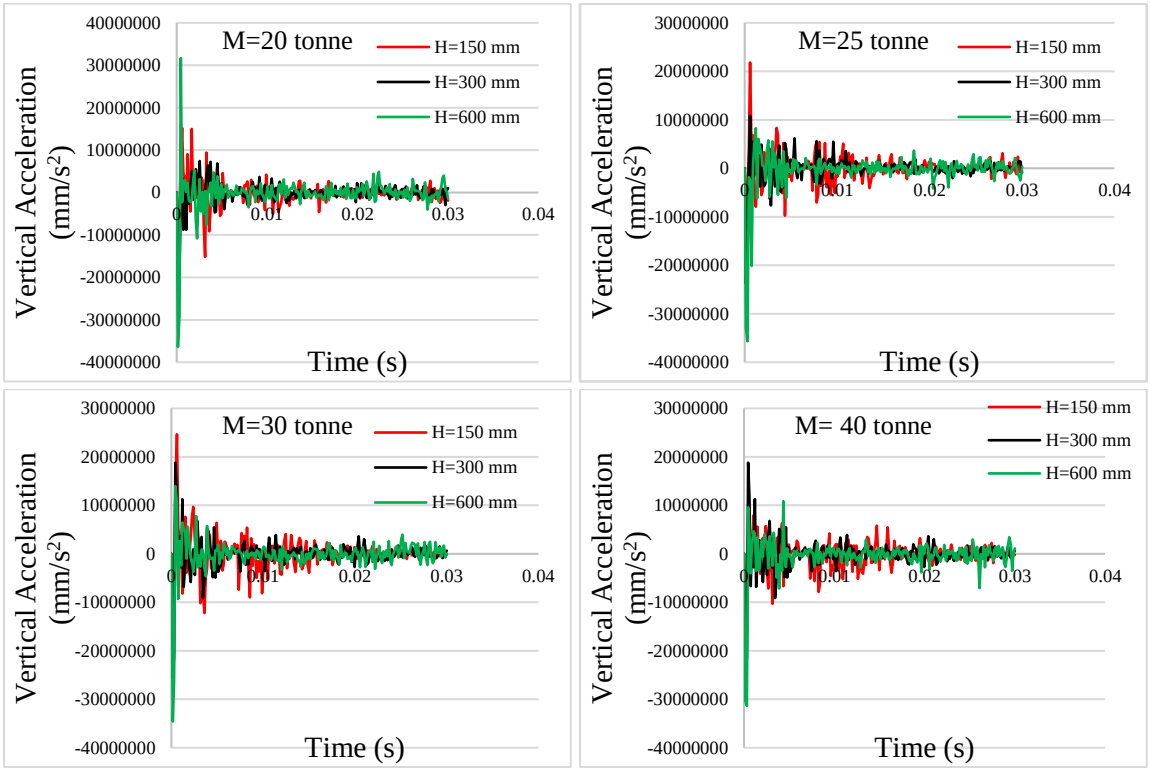

Figure 5.4 Midspan acceleration vs. time of steel for different masses and drop heights

The impact produces fluctuating acceleration which instantaneously increases to a peak value and then reaches to zero value followed by an instantaneous change in the direction of acceleration. The same pattern continues for a short duration of time with decay in the peak value of acceleration. The steel flange reaches the peak value of acceleration just after the impact.

The peak value of acceleration increases as the height of impact increase due to the increase in energy of impact as the drop height of impactor increases. Whereas, the increase in mass of impactor increases the residual acceleration i.e. increase in mass increases the time required for the decay of acceleration of steel flange. This behaviour may be because the increase in mass of impactor increases the time period of contact between the composite girder and the impactor.

The impacts with low energy tend to show larger post peak acceleration as compared to those of impacts with high energy. The mass of impactor does not seem to affect the peak value of acceleration significantly.

5.3.2 Variation of midspan acceleration at the top of the concrete slab

Following figures show the variation of midspan acceleration at the top of the concrete slab.

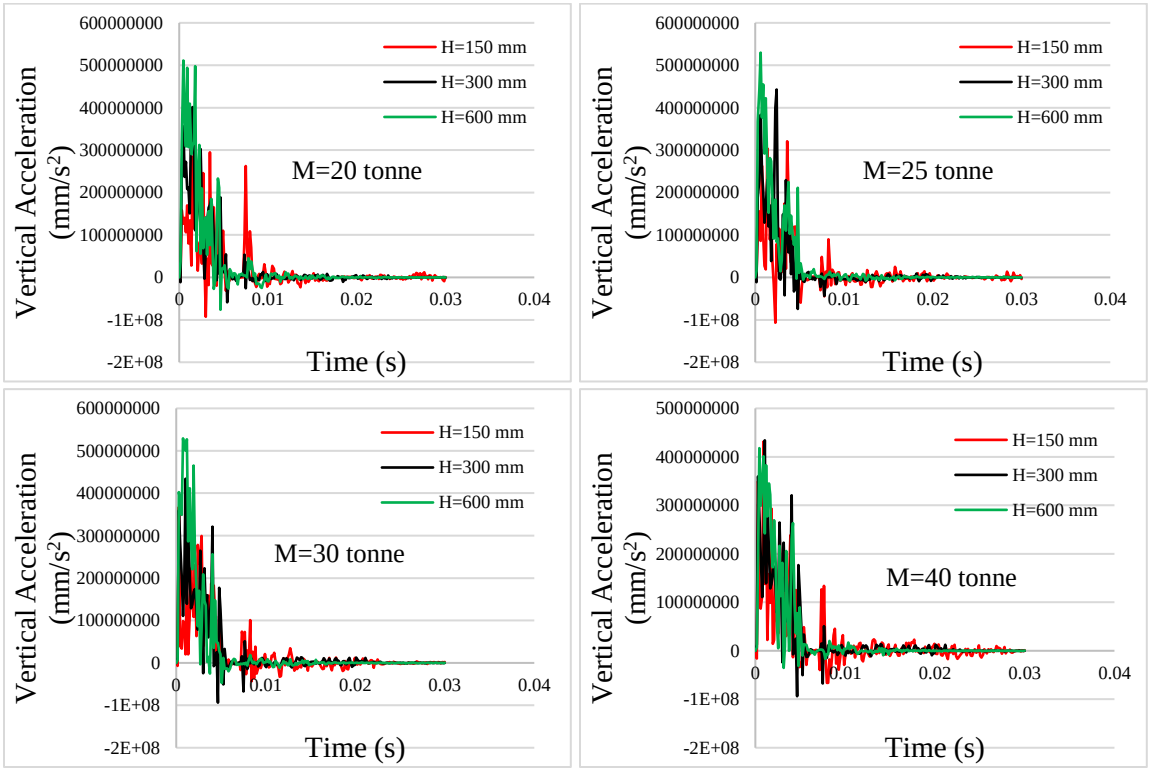

Figure 5.5 Midspan acceleration vs. time of concrete for different masses and drop heights

The top of the concrete slab is subjected to a larger magnitude of acceleration as than that of bottom steel flange as it is in the direct contact of the impactor. The acceleration of the concrete slab reaches a peak value shortly after impact followed by some low peaks and then it decays with time. In the initial stages of impact, the acceleration in concrete slab does not change direction contrary to that of bottom steel flange.

The peak value of acceleration increases with increase in the height of impact due to increase in the energy of impact. The increase in mass of impactor increases the time required for the decay of residual acceleration due to increased time period of contact between composite girder and impactor. Whereas, the decrease in mass or height of impact increases the magnitude of low peaks generated after the peak value of acceleration. Again, increase in mass of impactor does not cause large variation in the peak value of acceleration.

5.3.3 Variation of midspan velocity

Variation of midspan velocity at the bottom of steel flange is depicted through the following charts.

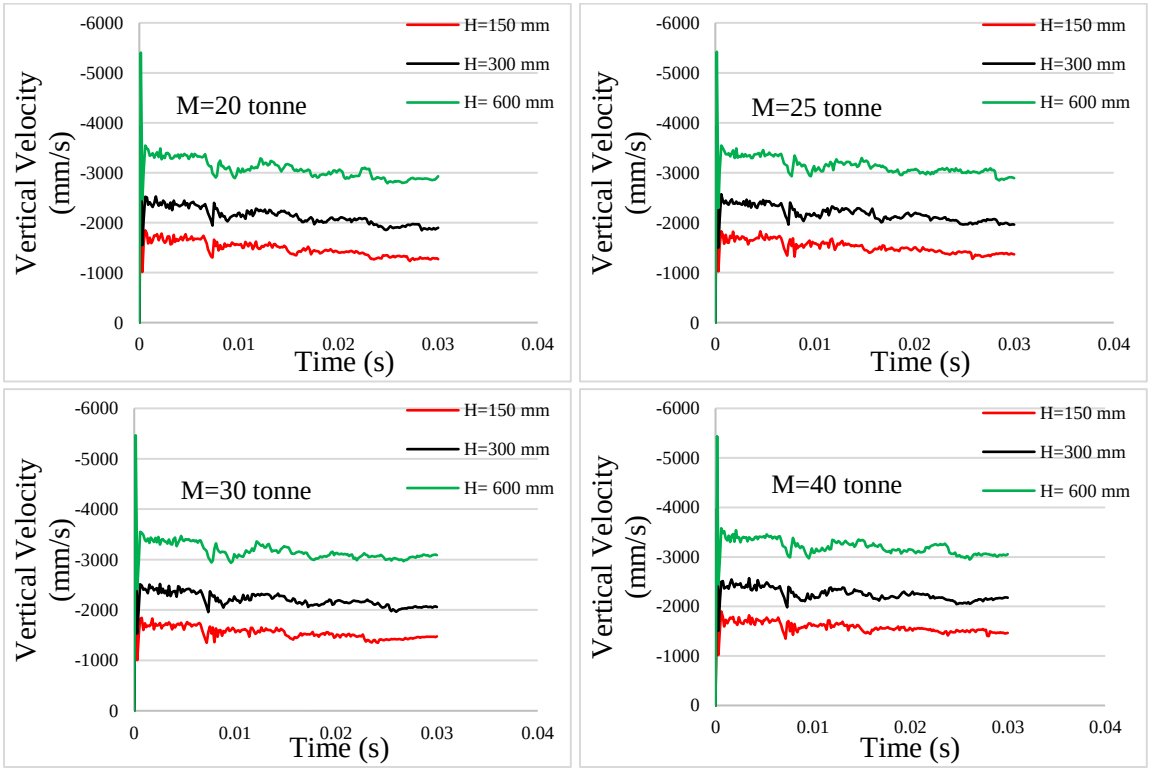

Figure 5.6 Midspan velocity vs. time for different for different masses and drop heights

A spiked increase in midspan velocity is observed instantaneously after the impact; further velocity decreases to the lowest value in a very short interval of time then an increase in velocity is observed after which it continues to decrease at a relatively slower rate with short spikes.

The midspan velocity of the girder is significantly affected by the height of impact as it increases by a large magnitude with increase in drop height of impactor. On the other hand, the mass of impactor does not have a noticeable effect on midspan velocity due to the fact very small increase in velocity is observed with increase in mass of impactor.

At the end of analysis time, midspan velocity attains almost constant value with a very slow rate of decay, as the midspan acceleration decays almost to zero.

5.3.4 Variation of midspan deflection

Following figures shows the variation of midspan deflection at the bottom of steel flange

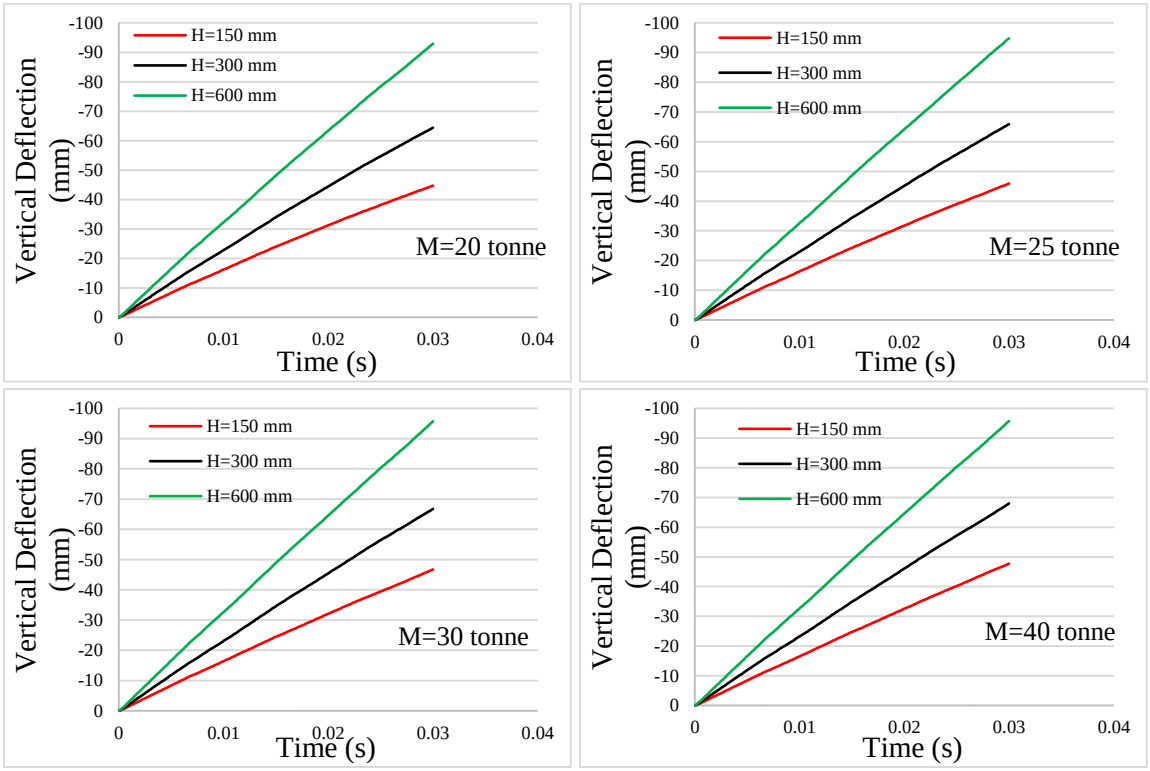

Figure 5.7 Midspan deflection vs. time for different masses and drop heights

From the above curve, it can be concluded that the variation of deflection with time is almost linear. The linear variation of deflection with time is observed because midspan velocity attains almost constant value in a very short interval of time. The rate of deflection increases with increase in the height of impact. Whereas, increase in mass of impactor has an insignificant effect on the midspan deflection.

Height/Mass	20 tonne	25 tonne	30 tonne	40 tonne
150 mm	45.9451	45.9131	46.74	47.7355
300 mm	64.3912	65.8962	66.7513	67.9849
600 mm	92.9164	94.7778	95.7168	97.0107

Table 5.2 Maximum values of deflection (mm) for varying mass and height of impactor

Midspan deflections in the case of impact loading at the end of 30 ms are increased by large magnitudes as compared to the case of static loading. The ultimate midspan deflection in case of impact loading is 2, 2.8, 4 times larger than that of in case of static loading for the drop heights to 150 mm, 300 mm, 400 mm respectively.

5.3.5 Variation of slip between concrete slab and steel flange

Following figures shows the variation of slip between concrete slab & steel flange at the end of the girder.

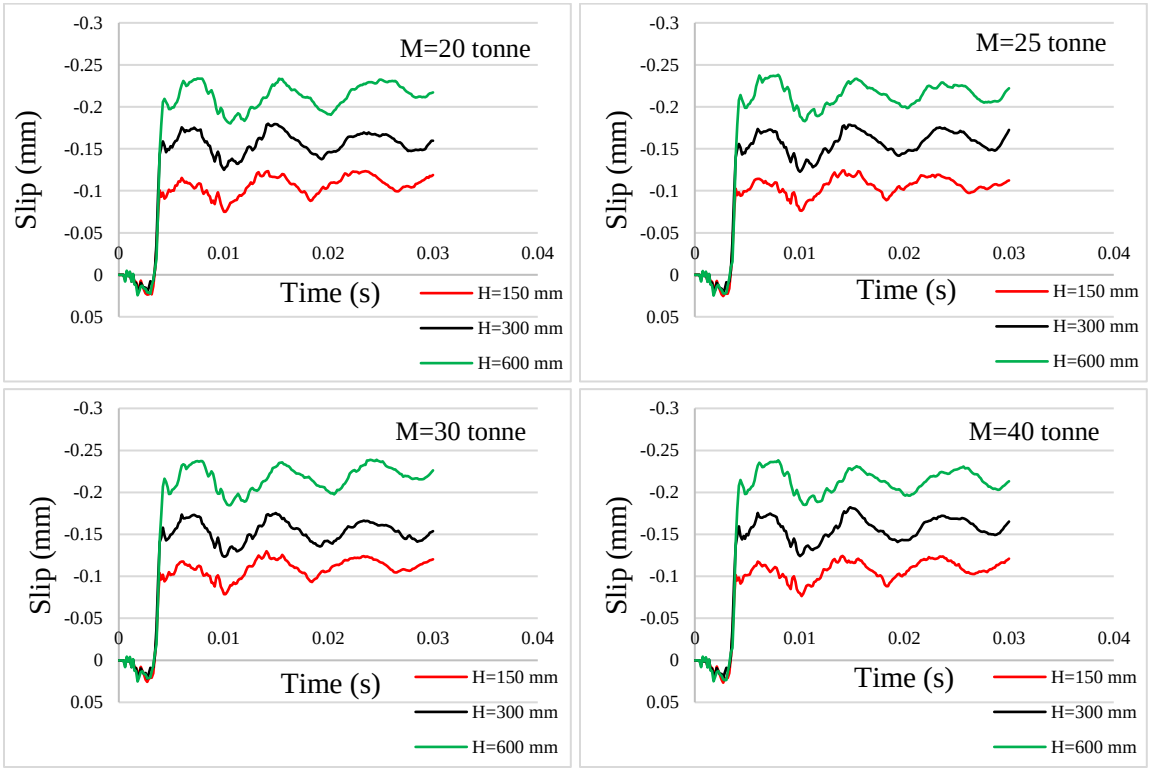

Figure 5.8 Slip vs. time for different masses and drop heights

The slip between concrete slab and steel flange is an indicator of the effectiveness of shear connection between steel and concrete. The direction of slip between concrete slab and steel flange is changed shortly after the impact. The relative between steel and concrete suddenly increases after changing direction. The magnitude of slip shows almost damped sinusoidal variation superimposed over a constant value. The amplitude of slip decays as with time, and a constant value may be attained after some time.

The overall magnitude of slip increases with increase in drop height. Whereas magnitude of slip almost remains unaffected by the increase in mass of impactor.

Height/Mass	20 tonne	25 tonne	30 tonne	40 tonne
150 mm	0.12347	0.12427	0.12998	0.12433
300 mm	0.17995	0.17857	0.17541	0.18229
600 mm	0.23378	0.23814	0.2388	0.23821

Table 5.3 Maximum values of slip (mm) for varying mass and height of impactor

When compared to static load case, impact load case shows a significant increase in the slip between steel and concrete. The peak value of slip observed for drop heights of 150 mm, 300 mm, 600 mm increases by 1.8, 2.6, 3.4 times respectively as compared than ultimate slip between steel and concrete for the case of a static load.

5.3.6 Variation of total vertical reaction

The variation of total vertical reaction with time is shown in the following figures.

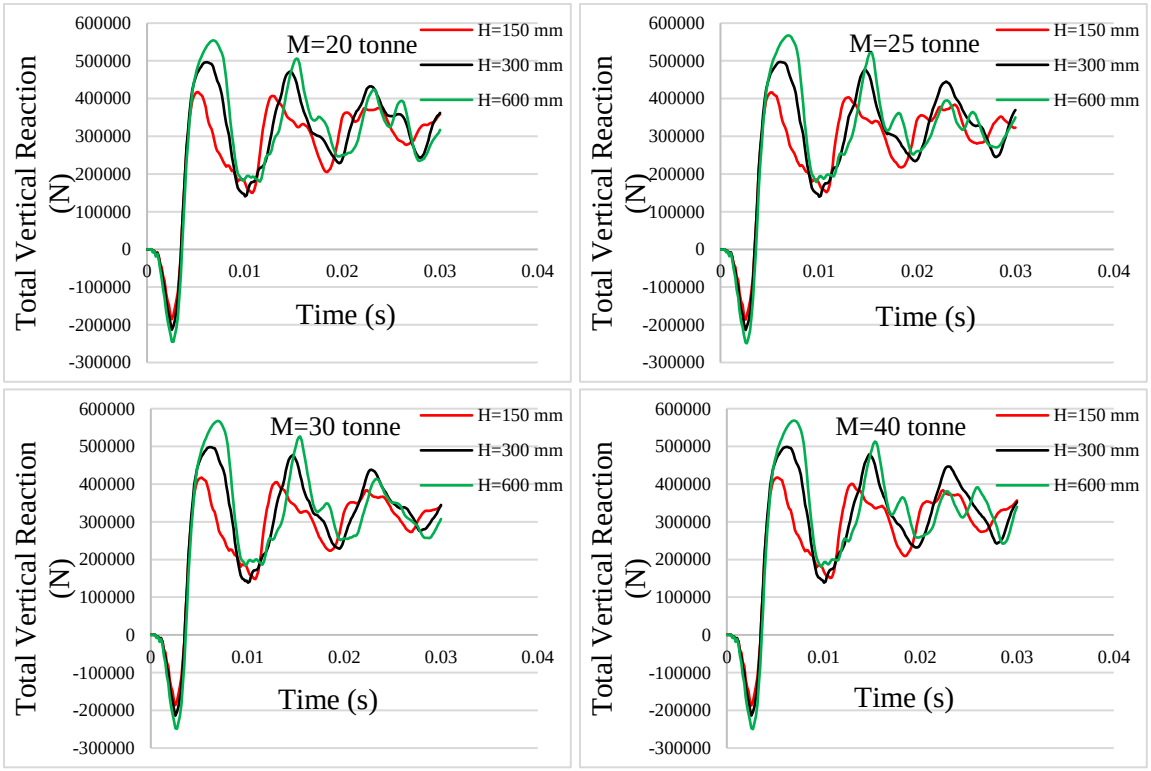

Figure 5.9 Total vertical reaction vs. time for different masses and drop heights

In the initial stage of impact downward reaction forces are observed. After a short interval of time, the direction of reactions is reversed, and a peak value is achieved which follows almost damped sinusoidal variation superimposed over a constant value. As the time increases the amplitude of reactions tends to decrease i.e. after sometime reactions may attain a constant value. This behaviour may be due to the wave propagation generated by the impact.

A Higher value of drop height of impact produces large variations in reactions as compared to than that of lower drop height of impact. Whereas, with an increase in mass of impactor the reactions are increased by a very insignificant amount.

Height/Mass	20 tonne	25 tonne	30 tonne	40 tonne
150 mm	416867.7	416490.5	417238.1	417596.2
300 mm	496368.8	496883.1	497973.5	498526.8
600 mm	554263.3	567583	567485.3	568376.2

Table 5.4 Maximum vertical reactions (N) for varying mass and height of impactor

Substantial increase in reactions is observed in the case of impact loading when compared to the case of the static load. The peak value of reactions observed is approximately 1.4, 1.6, 1.9 times for the drop heights of 150 mm, 300 mm, 600 mm respectively.

5.3.7 Variation of stress vs. strain curve at the midspan of the concrete slab

The following figure shows variation of Stress vs. Strain Curve at the Midspan of the Top of Concrete Slab is

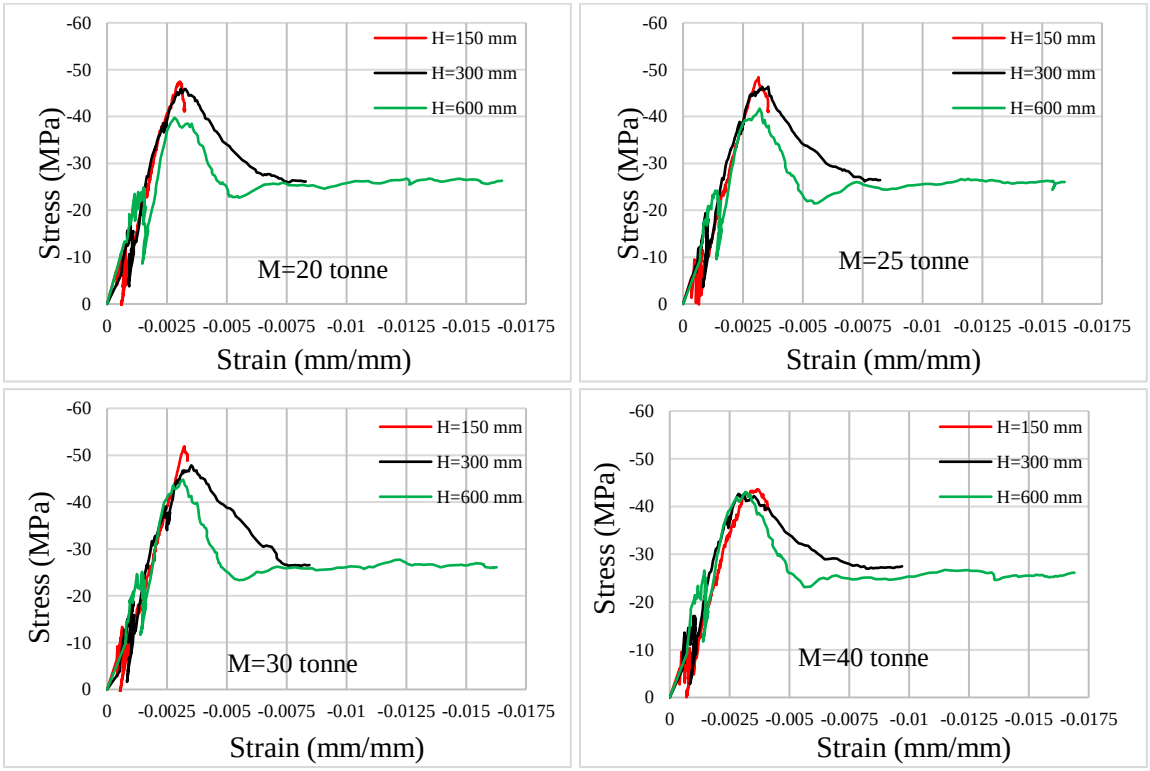

Figure 5.10 Stress vs. strain for concrete using different masses and drop heights

The stress vs. strain curve of concrete under impact typically follows stress vs. strain curve of concrete under uniaxial compression with some rapid fluctuations in stress at stress values lower than maximum stress in concrete.

From the above graph, it can be observed that the value of maximum stress decreases as the height of impact is increased i.e. concrete cracks at much lower stress when the height of impact is increased. As the mass of impactor is increased the difference in maximum stress achieved in concrete is reduced and concrete cracks at approximately same stress for all drop height of impact.

The stress vs. strain curve of concrete indicates the lower value of maximum strain achieved as the energy of impact is increased (by increasing mass and drop height of impact).

When compared to the static case of loading the maximum strain achieved in the case of impact loading is approximately 8.8 times higher than that of in case of static loading. Whereas, maximum stress achieved is 1.5 times higher than maximum stress achieved in the case of static loading.

5.3.8 Variation of stress vs. strain at the midspan of bottom steel flange

The variation of Stress vs. Strain at the Midspan of Bottom Steel Flange is shown in the following figure

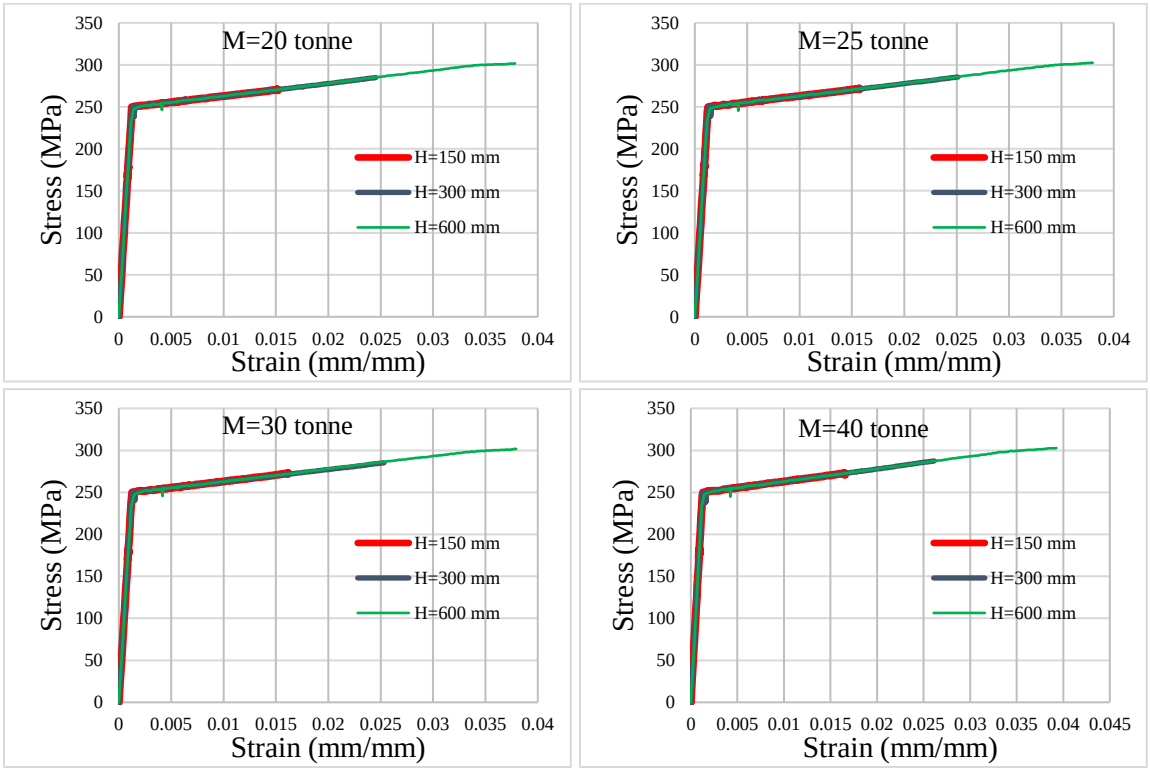

Figure 5.11 Stress vs. strain for steel using different masses and drop heights

The stress vs. strain curve for steel follow characteristic stress vs. strain curve of steel under uniaxial tension. From the above curves, it can be deduced that the steel is yielded in all the cases whether the mass of impactor is less than or greater than yield load of the girder under static load. The value of maximum strain increases with increase in energy of impact.

The maximum value of strain in case of impact loading is 5.4 times higher than that of static load case. The maximum value of stress achieved during impact is 1.2 times higher than the maximum stress achieved in static loading case.

CHAPTER 6

CONCLUSIONS

6.1 Conclusions

The methodology for the modelling and analysis for composite girder has been successfully developed and numerically validated. The same methodology has been applied on the representative girder. By investigating the different parameters obtained by the numerical simulation of composite girder under static and impact loading following conclusions can be drawn

- The capacity of the composite girder under static loading as calculated by rigid plastic analysis is higher than the ultimate load capacity obtained by finite element analysis of the same because materials fail fails before achieving ultimate stress as assumed in the theoretical analysis.
- The parameters such as midspan deflection, interfacial slip between steel and concrete, support reactions, stress and strain produced in concrete and steel are substantially increased in the case of impact loading when compared to parameters generated for the same magnitude of the static load.
- The concrete slab and steel flange are subjected to different magnitudes of vertical forces. This may be due to different magnitude of vertical acceleration experienced by steel and concrete. The peak value of acceleration increases as the energy of impact is increased at the same time the magnitudes of low peaks generated after peak value of acceleration is reduced with an increase in the energy of impact.
- Midspan deflection, interfacial slip between steel and concrete, support reactions, acceleration, velocity are more affected by drop height of impactor rather than a mass of impactor.
- Interfacial slip and support reaction show sinusoidal variation with time hence peak value must be taken into account for protective design consideration.
- Reversal of support reaction in the initial stages of impact is noteworthy which may cause failure of support if not taken into design consideration.
- The increase in the height of impactor causes cracking of concrete at lower stress and development of larger magnitude of strain before failure.
- The increase in the energy of impact causes the development of large magnitude of strain in concrete and steel.

6.2 Limitations of study

The investigations performed over composite girder under impact loading have following limitations.

- A parametric study of the steel-concrete composite girder under impact loading can be performed to see the effect of its details on its dynamic response after verification of numerical analysis of the same experimentally.
- The rebound mechanism may be included in the modelling of supports of composite girder.

APPENDIX-I: Rigid Plastic Analysis of Composite Girder

Calculations for plastic moment carrying capacity of the steel-concrete composite girder by rigid plastic analysis is shown below.

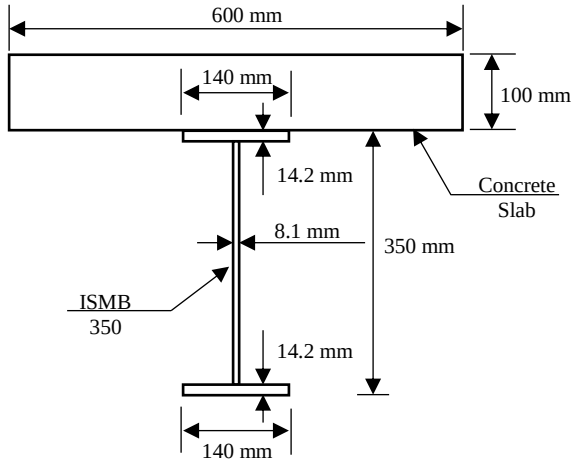

Figure 7.1 Sectional dimensions of steel-concrete composite girder

Cylindrical compressive strength of concrete (f_c) = 45 MPa

Yield strength of steel (f_y) = 250 MPa

Strength of concrete = Sectional area of concrete * 0.85 * f_c (7.1)

= 600 * 100 * 0.85 * 45

= 2295000 N

= 2295 kN

Strength of steel I-section = Sectional area of steel * f_y (7.2)

= (14.2 * 140 *2 + 8.1 * 321.8) * 250

= 1645240 N

= 1645.24 kN

∵ Strength of concrete > Strength of steel

∴ Compressive and tensile forces generated in the plastic state of section will be governed by strength of steel.

Effective depth of concrete in the plastic state = $\frac{\text{Strength of steel}}{\text{width of concrete} * 0.85 * f_c}$ (7.3)

$$= \frac{1645240}{600*0.85*45} = 71.69 \text{ mm}$$

Lever arm for plastic moment = 350/2 + 100 – 71.69/2

= 239.16 mm

Plastic moment carrying capacity = Lever arm * Strength of steel (7.4)

= 239.16 * 1645240

= 393475598.4 N-mm

= 393.48 kN-m

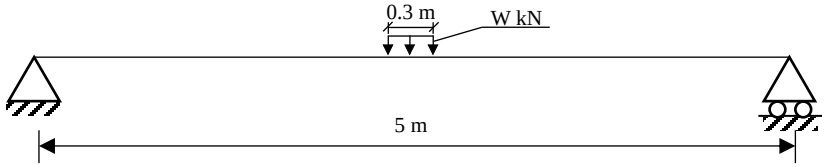

Figure 7.2 Line representation of loads on simply supported composite girder

By equating the maximum bending moment generated in the above beam to the plastic moment carrying capacity of the composite section, collapse load is calculated as

$$\frac{W}{2} * 2.5 - \frac{W}{2} * \frac{0.15}{2} = 393.48 \quad (7.5)$$

From the above equation collapse load W = 324.52 kN

APPENDIX-II: Design of Shear Studs and Slab Reinforcements

The design of shear studs in the group is shown below.

Strength of Studs in a group (Oehlers and Johnson 1987) is given by

$$\text{Strength (Dmax)} = K_{ch} * A_{sh} * f_u * \left(\frac{f_c}{f_u}\right)^{0.35} * \left(\frac{E_c}{E_s}\right)^{0.4} \quad (8.1)$$

Where,

$$K_{ch} = 4.7 - \frac{1.2}{\sqrt{N_{gr}}} \quad (8.2)$$

$$N_{gr}(\text{number of shear studs in a shearspan}) = \frac{\text{Strength of steel}}{D_{max}} \quad (8.3)$$

A_{sh} is the area of the shank of the shear stud.

f_u is the ultimate strength of stud.

f_c is the cylindrical compressive strength of concrete

E_c is modulus of elasticity of concrete

E_s is the modulus of elasticity of stud.

Available data,

$A_{sh} = \frac{\pi}{4} * 15.875^2 = 197.93$ mm^2

$f_u = 448.16$ MPa

$f_c = 45$ MPa

$E_c = 36.38$ GPa

$E_s = 209.187$ GPa

Trial 1,

For first trial assuming N_{gr} as infinity.

Using equation (8.2), $K_{ch} = 4.7$

Using equation (8.1), $D_{max} = 92639.57$ N

Trial 2,

Using equation (8.3), $N_{gr} = 17.76 \approx 18$

$K_{ch} = 4.7 - \frac{1.2}{\sqrt{18}} = 4.42$

$D_{max} = 87120.62$ N

Similarly, for trial 3,

$N_{gr} = 18.88 \approx 19$

$K_{ch} = 4.7 - \frac{1.2}{\sqrt{19}} = 4.42$

$D_{max} = 87120.62$ N

Similarly, for trial 4.

$N_{gr} = 18.88 \approx 19 = N_{gr}$ obtained in previous trial

$\therefore N_{gr} = 19$

Using two parallel rows of shear studs @ 260 c-c 10 in each row, total no of studs = 10*2*2

= 40

Check for spacings

Adopted spacing between rows = 80 mm $\geq 4 * d_{sh}$ (safe)

Adopted edge distance of studs = 30 mm $\geq 1.3 * d_{sh}$ (safe)

Adopted longitudinal spacing between studs = 260 mm $\geq 5 * d_{sh}$ (safe)

≤ 6 * depth of concrete (safe)

Calculation of reinforcement in the concrete slab is shown below.

Sectional area of longitudinal reinforcement (BIS 2000) = $0.85\frac{b*d}{f_y}$ (8.4)

$= 204\ mm^2$

Where,

b = width of concrete slab = 600 mm

d = Depth of concrete slab = 100 mm

f_y = yield strength of reinforcement = 250 MPa

using 5-8 mm ϕ bars, sectional area of reinforcement bars = 251.32 mm^2

The spacing for minimum shear reinforcement (BIS 2000) is given by

Spacing between of transverse stirrups = $\frac{A_{sv} * 0.87 * f_y}{0.4 * b}$ (8.5)

$= 91.1\ mm \approx 90\ mm$

Where,

b = width of concrete slab = 600 mm

A_{sv} = Sectional area of stirrup, using 2 legged-8 mm ϕ bars A_{sv} = 100.53 mm^2

f_y = yield strength of reinforcement = 250 MPa

Spacing adopted for transverse stirrup = 90 mm

References

Baskar, K., and Shanmugam, N. (2003). "Steel–concrete composite plate girders subject to combined shear and bending." *Journal of Constructional Steel Research*, 59(4), 531-557.

BCSA, life, S. f., and SCI (2001). "Composite construction." <http://www.steelconstruction.info/Composite_construction>. (10 March, 2017).

BCSA, life, S. f., and SCI (2001). "Shear connection in composite bridge beams - Steelconstruction.info." <http://www.steelconstruction.info/Shear_connection_in_composite_bridge_beams>. (2017, 10 March).

BIS (1964). "Handbook for Structural Engineers SP:6(1)." *Rolled Steel Sections* New Delhi.

BIS (2000). "456: 2000,—Plain and reinforced concrete code of practice‖ Bureau of Indian Standards." *Fourth revision*.

Boyer, H. E. (1987). "Atlas of Stress--strain Curves." *ASM International, Metals Park, Ohio 44073, USA, 1987. 630*.

Carreira, D. J., and Chu, K.-H. (1985). "Stress-strain relationship for plain concrete in compression." *ACI Journal*, 82(6), 797-804.

Carreira, D. J., and Chu, K.-H. (1986). "Stress-strain relationship for reinforced concrete in tension." *ACI Journal*, 83(1), 21-28.

Chen, W. F. (1988). "Da Jian Han. Plasticity for Structural Engineers." New York: Springer· Verlag.

Committee, A., Institute, A. C., and Standardization, I. O. f. "Building code requirements for structural concrete (ACI 318-08) and commentary." American Concrete Institute.

Deng, L., Wang, W., and Yu, Y. (2015). "State-of-the-art review on the causes and mechanisms of bridge collapse." *Journal of Performance of Constructed Facilities*, 30(2), 04015005.

Foley, C. M., and Vinnakota, S. (1997). "Inelastic analysis of partially restrained unbraced steel frames." *Engineering structures*, 19(11), 891-902.

Hawkins, N. M., and Mitchell, D. (1984). "Seismic response of composite shear connections." *Journal of Structural Engineering*, 110(9), 2120-2136.

Hegger, J., and Rauscher, S. "Innovative shear connection for composite beams with UHPC." *Proc., 2nd international symposium on connections between steel and concrete*, 1295-1204.

Hibbitt, Karlsson, and Sorensen (2013). *Abaqus 6.13 Online Documentation*, Dassault Systèmes.

Higgins, C., and Mitchell, H. (2001). "Behavior of composite bridge decks with alternative shear connectors." *Journal of Bridge Engineering*, 6(1), 17-22.

Jurkiewiez, B., Meaud, C., and Michel, L. (2011). "Non linear behaviour of steel–concrete epoxy bonded composite beams." *Journal of Constructional Steel Research*, 67(3), 389-397.

Kaewunruen, S., and Remennikov, A. (2007). "Low-velocity impact analysis of railway prestressed concrete sleepers."

King, D. C., Slutter, R. G., and Driscoll, G. C. (1965). "Fatigue strength of 1/2-inch diameter stud shear connectors." *Highway Research Record*(103).

Kmiecik, P., and Kamiński, M. (2011). "Modelling of reinforced concrete structures and composite structures with concrete strength degradation taken into consideration." *Archives of civil and mechanical engineering*, 11(3), 623-636.

Kumar, P., Chaudhary, S., and Gupta, R. (2017). "Behaviour of Adhesive Bonded and Mechanically Connected Steel-concrete Composite under Impact Loading." *Procedia Engineering*, 173, 447-454.

Kupfer, H. B., and Gerstle, K. H. (1973). "Behavior of concrete under biaxial stresses." *Journal of the Engineering Mechanics Division*, 99(4), 853-866.

Liang, Q. Q., Uy, B., Bradford, M. A., and Ronagh, H. R. (2004). "Ultimate strength of continuous composite beams in combined bending and shear." *Journal of Constructional Steel Research*, 60(8), 1109-1128.

Louw, J., van Dyk, A., and Roux, A. (1970). "Stud Shear Connectors In Composite Steel And Concrete Construction Under Impact." *WIT Transactions on The Built Environment*, 8.

Oehlers, D., and Johnson, R. (1987). "The strength of stud shear connections in composite beams." *The Structural Engineer*, 65(2), 44-48.

Pavlović, M., Marković, Z., Veljković, M., and Buđevac, D. (2013). "Bolted shear connectors vs. headed studs behaviour in push-out tests." *Journal of Constructional Steel Research*, 88, 134-149.

Pham, T. M., and Hao, H. "Review of concrete structures strengthened with FRP against impact loading." *Proc., Structures*, Elsevier, 59-70.

Remennikov, A. M., Kong, S. Y., and Uy, B. (2010). "Response of foam-and concrete-filled square steel tubes under low-velocity impact loading." *Journal of Performance of Constructed Facilities*, 25(5), 373-381.

Shariati, A., RamliSulong, N., and Shariati, M. (2012). "Various types of shear connectors in composite structures: A review." *International Journal of Physical Sciences*, 7(22), 2876-2890.

Simulia, D. (2013). "ABAQUS 6.13 User's manual." *Dassault Systems, Providence, RI*.

Song, H.-W., You, D.-W., Byun, K.-J., and Maekawa, K. (2002). "Finite element failure analysis of reinforced concrete T-girder bridges." *Engineering Structures*, 24(2), 151-162.

Thevendran, V., Chen, S., Shanmugam, N., and Liew, J. R. (1999). "Nonlinear analysis of steel–concrete composite beams curved in plan." *Finite Elements in Analysis and Design*, 32(3), 125-139.

Viest, I. "Investigation of stud shear connectors for composite concrete and steel T-beams." *Proc., Journal Proceedings*, 875-892.

Wahalathantri, B. L., Thambiratnam, D., Chan, T., and Fawzia, S. "A material model for flexural crack simulation in reinforced concrete elements using ABAQUS." *Proc., Proceedings of the First International Conference on Engineering, Designing and Developing the Built Environment for Sustainable Wellbeing*, Queensland University of Technology, 260-264.

Wang, Y. (1998). "Deflection of steel-concrete composite beams with partial shear interaction." *Journal of Structural Engineering*, 124(10), 1159-1165.

Zheng, Y., Robinson, D., Taylor, S., and Cleland, D. (2009). "Finite element investigation of the structural behaviour of deck slabs in composite bridges." *Engineering Structures*, 31(8), 1762-1776.

Zineddin, M. (2008). "Simulation of reinforced concrete slab behavior under impact loading." *AEI 2008: Building Integration Solutions*, 1-9.

Finite Element Analysis of Simply Supported Steel-Concrete Composite Girder Under Impact Loading

ORIGINALITY REPORT

%15	%6	%12	%2
SIMILARITY INDEX	INTERNET SOURCES	PUBLICATIONS	STUDENT PAPERS

PRIMARY SOURCES

1	abaqus.ethz.ch:2080 Internet Source	%1
2	A. Kumar. "Measurement of Rain-Induced Zenith-Path Attenuation Using 19.9 GHz Radiometer at Amritsar (India)", IEEE Transactions on Antennas and Propagation, 3/2004 Publication	%1
3	Remennikov, Alex M., Sih Ying Kong, and Brian Uy. "Response of Foam- and Concrete-Filled Square Steel Tubes under Low-Velocity Impact Loading", Journal of Performance of Constructed Facilities, 2011. Publication	%1
4	Thevendran, V.. "Nonlinear analysis of steel-concrete composite beams curved in plan", Finite Elements in Analysis & Design, 199906 Publication	%1
5	academicjournals.org Internet Source	